Particle Swarm Optimization (PSO) Based PID Speed Control of BLDC Motor Drive with Regenerative Breaking for Electric Vehicle Application

Sintayehu Anagaw Minuye

A Thesis Submitted to

The Department of Electrical Power and Control Engineering

School of Electrical Engineering and Computing

Presented in Partial Fulfillment of the Requirement for the Master of Science Degree in Electrical Power and Control Engineering (Specialization in Control Engineering)

Office of Graduate Studies

Adama Science and Technology University

September, 2021

Adama, Ethiopia

Particle Swarm Optimization (PSO) Based PID Speed Control of BLDC Motor Drive with Regenerative Breaking for Electric Vehicle Application

Sintayehu Anagaw Minuye

Advisor: Dr. Tefera Terefe

A Thesis Submitted to
The Department of Electrical Power and Control Engineering
School of Electrical Engineering and Computing

Presented in Partial Fulfillment of the Requirement for the Master of Science Degree in Electrical Power and Control Engineering (Specialization in Control Engineering)

Office of Graduate Studies
Adama Science and Technology University

August 2021
Adama, Ethiopia

DECLARATION

I hereby declare that this Master Thesis entitled "Particle Swarm Optimization (PSO) Based PID Speed Control of BLDC Motor Drive with Regenerative Breaking for Electric Vehicle Application" is my original work. That is, it has not been submitted for the award of any academic degree, diploma, or certificate in any other university. All sources of materials that are used for this thesis have been duly acknowledged through citation.

Sintayehu Anagaw Minuye ______________ ____________________

Name of the student Signature Date

RECOMMENDATION

I, the advisor of this thesis, hereby certify that I have read the revised version of the thesis entitled “Particle Swarm Optimization (PSO) Based PID Speed Control of BLDC Motor Drive with Regenerative Breaking for Electric Vehicle Application” prepared under my guidance by Sintayehu Anagaw Minuye submitted in partial fulfillment of the requirements for the degree of Master of Science in Control Engineering. Therefore, I recommend the submission of the revised version of the thesis to the department following the applicable procedures.

Dr. Tefera Terefe	________________	__________________
Advisor	Signature	Date

APPROVAL OF BOARD OF EXAMINERS

I, the advisor of the thesis entitled "Particle Swarm Optimization (PSO) Based PID Speed Control of BLDC Motor Drive with Regenerative Breaking for Electric Vehicle Application" and developed by Sintayehu Anagaw Minuye, hereby certify that the recommendation and suggestions made by the board of examiners are appropriately incorporated into the final version of the thesis.

Advisor	Signature	Date

We, the undersigned, members of the Board of Examiners of the thesis by Sintayehu Anagaw Minuye have read and evaluated the thesis entitled "Particle Swarm Optimization (PSO) Based PID Speed Control of BLDC Motor Drive with Regenerative Breaking for Electric Vehicle Application" and examined the candidate during the open defense. This is, therefore, to certify that the thesis is accepted for partial fulfillment of the requirement of the degree of Master of Science in Control Engineering.

Chairperson	Signature	Date
Internal Examiner	Signature	Date
External Examiner	Signature	Date

Finally, approval and acceptance of the thesis is contingent upon submission of its final copy to the Office of Postgraduate Studies (OPGS) through the Department Graduate Council (DGC) and School Graduate Committee (SGC).

Department Head	Signature	Date
School Dean	Signature	Date
Office of Postgraduate Studies, Dean	Signature	Date

ACKNOWLEDGEMENTS

First, my hearty gratitude goes to the almighty God. Then I am highly grateful to my advisor Dr. Tefera Terefe, as with his encouragement, insight, and guidance the completion of this work would not have been possible. I also give great gratitude to Prof Gang Gyoo Jin for his initiation and open-mindedness.

Next, my honorable gratitude goes to my friends, for their help for finishing this thesis work.

Finally, I want to give great gratitude to, Department Head Mr. Mesfin Merga and department Postgraduate Coordinator Dr. Milkias Brhanu for their initiation for accomplishing the thesis in proper time.

ABSTRACT

The combustion of fossil fuels, a non-renewable and finite resource, has exacerbated air pollution, ozone damage, acid rain, and global warming. Fast depletion of energy resources reminds the importance of energy conservation. Combustion engine vehicles are responsible for more than 90% of the world global warming rate. A motor delivers only around 30 to 35% of the input energy. Electric vehicles are alternative solutions in order to reduce environmental air pollution due to fossil fuel driven vehicles. However, energy utilization and efficiency are the major issues in electric vehicles apart from the role of reducing air pollution. Energy has also wasted within the sort of heat whenever the brake is applied. But experience has indicated that the advantages don't seem to be always as great as may be expected due to inefficiencies within the power conversion processes. Extra mass and price can frequently restrict the financial feasibility of an electric vehicle with regenerative braking. Regenerative braking systems for electric vehicles enable the range of the vehicle be extended. In this thesis, the energy storage device, converters, battery, speed control of BLDC motor by multi-optimal approach of PSO, and regenerative brake are basically modelled and analysed mathematically using wheel dynamics equations. The simulation model was established under the circumstance of MATLAB/SIMULINK and script according to the speed control of BLDC motor by PSO-PID controller model, braking pedal intensity, and battery state of charge (SOC) for BEV are simulated and analysed. The simulation results have shown that, the recharging of battery or energy recovered during regenerative braking when the speed decrease, torque, and current are negative the distance range of BEV increase in one time charging under normal condition.

Keywords: *BLDC, Electric Vehicle, PID, and PSO*

TABLE OF CONTENTS

LIST OF TABLES

LIST OF FIGURES

ACRONYMS

AMC	American Motor Car Company
BEMF	Back Electromotive Force
BEV	Battery Electric Vehicle
BLDC	Brushless DC
DC	Direct Current
EMF	Electromotive Force
EV	Electric Vehicles
FLC	Fuzzy Logic Controller
HEV	Hybrid Electric Vehicles
IAE	Integral Absolut Error
ICE	Internal Combustion Engine
IGBT	Insulated-Gate Bipolar Transistor
IM	Induction Motor
Li-ion	Lithium-Ion Battery
Li-S	Lead-Acid
MATLAB	Matrix Laboratory
MOSFET	Metal Oxide Silicon Field Effect Transistor
Ni-cd	Nickel Cadmium
Ni--MH	Nickel-Metal Hydride
PI	Proportional Integral
PID	Proportional Integral Derivative
PMDC	Permanent Magnet Dc
PMSM	Permanent Magnet Synchronous Motors
PSO	Particle Swarm Optimization
PWM	Pulse Width Modulation
RBS	Regenerative Braking System
SOC	State Of Charge
SRM	Switched Reluctance Motor
HPSS	Hybrid Power
VSI	Voltage Source Inverter

LIST OF SYMBOLS

Symbol	Meaning	Unit
C_d	Aerodynamic drag coefficient	
ρ	Air density	(kg/m^3)
e_a, e_b, and e_c	Back-EMF	V
B	Damping constant	(N.m.s)
V_{dc}	Dc link voltage input	(V)
T_r	Delay time	Sec
A_f	frontal cross-sectional area	(m^2)
η	Efficiency	(%)
θ_r	Electrical rotor angle	(°)
E	Error	
λ_p	Flux linkage	(Wb)
B	Friction coefficient	(N)
G	Gravity	(m/s^2)
E_a, E_b, and E_c	Induced Back EMF	
J	Inertia	($kg.m^{2)}$
$\boldsymbol{T_L}$	Load torque	(N-m)
M	Mass	(kg)
V_{cm}	Maximum control voltage	(V)
ω_m	Mechanical speed of the rotor	(rad/s)
M	Mutual inductance per phase	(H)
P	Power	(kW)
I	Reference current amplitude	(A)
i_a, i_b, i_c	Reference phase currents	(A)
β	Road gradient angle	(°)

C_r	Rolling resistance coefficient	
$f_{a,b,c}(\theta_r)$	Rotor angle functions	
J	Rotor inertia	(kgm^2)
Θ	Rotor position	(°)
ω_m	Rotor speed	Rpm
L	Stator inductance per phase	(H)
$V_{a,b,c}$	Stator per phase stator voltages	(V)
R	Stator resistance per phase	(R)
Fc	Switching (carrier) frequency	(Hz)
K_t	Torque constant	(N-m/A)
V_x	Vehicle speed	(m/s)
v_{wind}	Wind speed	(m/s)

CHAPTER ONE

INTRODUCTION

1.1. Background

In these 21-century technologies growing up in every aspect, like development of electrical Vehicles is speeding up. EV's future will lie on the event of electrical, mechanical and control technology. Recently, electric vehicles driven by motor and also the key technology like control technology and integrative technology are put into application. However, the innovation of storage battery is not in practice, long battery charging time, huge expense and driving range is the vital limitation for the improvement of electric vehicles.

Automakers have put forth an extraordinary attempt to discover green, energy saving and zero pollution transportation devices. In this way, [1][2]. Powerful battery usage and progressed motor control have become a significant issue for EVs [3][4]. A PEV (pure electric vehicle) contains three significant parts: the force battery pack, the driving motor such as IM, BLDCM and SRM [4], etc.], and the DC-DC power converter. Brushless direct-current (DC) motor superior advantage than other motors which are brush DC motors, IMs and switching reluctance machine. It has the benefits of straightforward construction, high proficiency, electronic commutating device, high beginning force, less noise operation and huge speed range, and so on Subsequently, the brushless DC motor has been broadly utilized in EVs [5]. Conventional EVs utilize mechanical brakes to expand the friction of the wheel for deceleration purposes. In this manner, the slowing down kinetic energy is lost in the form of heat. In light of this issue, this paper will talk about how to change over the kinetic energy into electrical energy that can be re-energized or recharge to the battery pack, control the speed of BLDC motor through PID tune by the particles warm algorithm (PSO), current control by hysteresis control.

From the previously mentioned state of charge on regenerative braking these innovations may be categorized as :(1) regenerative braking is realized by utilizing the external energy storing components (ultra-capacitor pack) to soak up the instantaneous braking energy. In this way the battery pack and ultra-capacitor frame a crossover control supply framework HPSS additionally the depictions of HPSS are frequently found in [17–19]: (2) so as Energies to enhance the DC-link voltage of the ability converter, a bidirectional DC-DC power converter is employed for enhancing control [20,21]; (3) braking energy is recovered by using the driving power converter itself for charging control the energy recovery control is accomplished by utilizing distinctive control technique . [22,23]. For Classification (1), the extra energy-putting away parts should be charged and released through a DC-DC power converter, status of the ultra-capacitor (like full charged or under-voltage) should be procured, hence, voltage and current sensors should be introduced in the controller, thus, the slowing down energy is briefly put away in the ultra-capacitor pack.

For Classification (2), since the back electromotive force (BEMF) is a lot of lower than the battery's terminal voltage, even at high velocity, in this manner, the BEMF likewise should be supported for charging the battery pack. A portion of the controllers accomplish this objective by adding an extra buck-support regulator. The most ideal way, as we would see it, to understand this objective, is by utilizing the controller itself.). To beat the impediments of electric vehicles, the use of regenerative slowing down strategy which controls electrical motors worked as generators to change over motor or likely energy into electric energy that can be put away in the energy stockpiling gadgets, for example, super capacitors and batteries is a powerful way.in which rotational motion generated through the attraction and repletion of magnetic pole of permanent magnet and electromagnets. These motors are, however, operated in a totally different way. To convert DC power into three phase voltages, BLDCs require a sophisticated controller. A DC voltage may easily operate a brushed motor.

BLDC motor is more applicable device for light waited electric vehicle with their regenerative innovation of EV, under confirmation of slowing down security and dependability, whose capacity is to change over piece of mechanical energy into electric energy during slowing down by the regenerative stopping mechanism and store in an energy stockpiling device. So, it plays an important role in reducing the energy consumption of EV, extending the driving range and improving its economic performance and increase the distribution to the community. So, I design a regenerative braking force which is based on PSO-PID controller, which has three inputs including the driver’s required braking force (brake pedal), vehicle speed (BLDC motor speed) and battery SOC.

An electric vehicle is seen to cut back fuel consumption, improve overall drive system efficiency together with improving the drivability. Additionally, to any or all these facts other important issue is to own a correct model of the electrical vehicle so as to be ready to estimate the particular energy consumption which is incredibly well disbursed in. Regardless of these factors, electric cars still have a number of important challenges that need to be addressed. The restriction of the car's battery package is one of the primary problems of electric cars.

The battery bundle is required to at the same time have two properties first it ought to contain adequate energy for having a particular practice range and secondly It ought to too have a adequate control capability for the continual accelerations and decelerations. The major parameter, power, must be regulated for the electrical vehicle to function well; hence, the notion of a battery management system exists (BMS). The fundamental points of this work is to build up an electric vehicle model, PSO-PID BLDC motor speed control, recreate it, and break down the impact of energy the board technique utilized for the two cycles, forward driving and regenerative slowing down. The outcome demonstrated that energy recuperating proficiency of BEV in regenerative stopping mechanism for electric vehicles.

1.2. Problem of the Statement

In electric vehicles braking is one of the important aspects. The mechanical braking system which we use in our vehicles has a big drawback of wasting the kinetic energy of the vehicle as heat. This brings down the overall efficiency of the vehicle by affecting the fuel economy. In the urban drive cycle, we tend to start and stop the vehicle more often when compared to highway drive cycle. As we apply the brake often in an urban drive cycle, the energy loss is more. Generally, there are three main problems in overall world on BEV which are technological problem such as wasting the kinetic energy of the vehicle as heat, shorter driving ranges and take a long time to recharge.

Social problem such as social acceptance and Insufficient charge stations. Economic problem which is high price.

This thesis work will solve technological problems by develop regenerative braking on electric vehicle by adjusting BLDC motor speed control, reducing torque ripple and current performance and state of charge and discharge.

1.3. Objectives

1.3.1. General Objectives

Modelling, Designing and analysing of PSO-PID speed controller for BLDC motor with regenerative braking for electric vehicle.

1.4.2. Specific Objective

The specific objective of the studies is -

- To model three phase BLDC motor drive suitable for Electric Vehicle.
- To reduce kinetic energy loss when brake is applied on BEV.
- By recharge the battery and reuse its energy increase the vehicle travelled distance in one time charging process.
- To control the speed of the BLDC motor with regenerative braking system using MATLAB simulation tool.
- To decide the better optimization algorithm method for PID controller.

1.4. Significant of the Study

For sustainable transportation, recovering kinetic energy of electric vehicle that has been lost during braking system, improving the speed controller performance parameters of BLDC motor, decrease the air pollution, increase production of EV, increase stable energy flow and less utilize of conventional vehicle.

1.5. Motivation of the Study

As the global economy strives towards clean energy in the face of climate change; the automotive industry is researching into improving the efficiency of automobiles. Electric Vehicles (EV) are an answer to the crisis the world is about to face in the near future. But the address that's being continuously inquired is how can the driving extend of electric vehicles be increased. The answer to this question lies within the success of the investigate for an efficient and power packed energy source like an enchantment battery or success with fuel cells, efficient regenerative braking systems, etc. In regenerative braking, the kinetic energy can be changed over back into electrical energy that can be stored in batteries for reuse to move the vehicle [5]. In this manner, regenerative braking has potential to moderate energy which can improve fuel economy whereas reducing emissions that contribute to air pollution.

1.6. The Scope of the Study

Regenerative braking frameworks require advance research to create better system that captures more energy and stops quicker in short distance. So, these systems will become more and more common. In this work, a BLDC motor is used which is going to be controlled by PSO PID controller. All vehicles in motion can like these systems by recapturing energy that may are lost during braking process. Future innovations in regenerative brakes will incorporate modern types of motors which is able to be more proficient as generators modern drive prepare designs which is built with regenerative braking in intellect and electric systems which can be less helpless to energy losses.

1.7. Limitation of the Study

The thesis is limited to the simulation of the system using MATLAB/Simulink by showing how the different components of the system interact with each other. Analysis of torque ripple minimization is not done. The implementation of the real system is difficult because of the materials availability in the country. Along with it takes the additional time and cost incurred to making the actual prototype implementation

1.8. Organization of the Study

Chapter 1: The first chapter presents the introduction of BLDC motor drive and regenerative braking system in electric vehicle, Chapter 2: Reviewed literatures and papers on the background. And also cover advantage of BLDC motor compared with the other electric motors and existing control mechanism of BLDC motor are discussed. Chapter 3: Covers the investigation of BEV model description and calculation of force from their specification, BLDC motor drive modeling and the proposed system controller are explained. Chapter 4: The proposed system results are discussed in chapter four. Chapter 5: Finally, conclusion and recommendation are made in chapter five.

CHAPTER TWO

BASIC THEORY AND LITERATURE REVIEW

2.1. Chapter Overview

In this chapter unique electric vehicle models with their motors and regenerative slowing down BEV for energy recuperation system are looked into. The overall application spaces of BLDC motor, the current controlling component, the driving techniques, for regenerative braking of BEV and other related uses of BLDC motor are examined. Firmly related works particularly in regenerative stopping mechanism in EV with various control system and speed control of brushless DC motor are inspected and discussed.

2.2. Electric Vehicle

The world most important thing for transportation purpose is Electric vehicle, but rather with the creative movement and expanded worry on controlling contamination have given it a tag of future portability. In EV's, electric energy is the most wellspring of force for drive of a vehicle. In electric vehicles electrical energy is changed over into mechanical rotational energy by electric motors. This rotational energy is associated with the wheels of a vehicle through a proper transmission framework which thus causes drive. A vehicle with four engines can be considered as the chief productive show in electric vehicles. Electric vehicles can use electric energy as a sole wellspring of force or can use batteries related to gas motors to control the vehicle. Battery, electric engine and regulator are the center segments of any electric vehicle.

2.2.1. Types of Electric Vehicle

The fundamental energy source of electric vehicle is battery, yet there are sorts that can utilize other fuel source mod is called cross breed EVs (HEVs). The Worldwide Electro Specialized Commission's Specialized Advisory group 69 (Electric Street Vehicles) suggested that vehicles utilizing at least two kinds of fuel Source stockpiling or converters can be called as a HEV as long as at any rate one of those generate electrical vitality [4]. This definition shows a great deal of mixes feasible for HEVs like ICE and battery, battery and ultra-capacitor-helped EVs [7].

EVs can be classified as: - Battery Electric Vehicle, Hybrid Electric Vehicle (HEV), Plug-in Hybrid Electric Vehicle (PHEV) and Fuel Cell Electric Vehicle (FCEV)

❖ Battery Electric Vehicle (BEV)

- Nissan Leaf
- Tesla Model S
- BMW i3

I choose BMWi3 electric vehicle for this thesis to appropriate use in BLDC motor application and the main specification is listed follow in the figure 2.1.

Figure 2. 1 BMW i3 [7]

- Variant: BMW i3 (120 Ah)
- 42.2 kWh lithium-ion (Li-ion) battery
- Fast charging (125A, 80% SOC: under 40 min.)
- Normal charging (60A, 80% SOC: 7.5 hours)
- 11kW, 352 V onboard charger three phase 16A
- 125kW AC motor, 250 Nm maximum torque
- Range up to 300 km
- Mass 1345kg
- with drag coefficient of 0.3
- 5 seats

Table 2. 1 Comparison of different Electric vehicle types[8]

EV type	Driving component	Energy source	Features	Problems
BEV	Electric motor	Battery Ultra-capacitor	No emission Not dependent on oil Range is dependent largely on the type of battery used Available commercially	Battery price & capacity Range Charging time Availability of charging stations High price
HEV	Electric motor ICE	Battery Ultra-capacitor ICE	Very little emission dependent on oil Long range battery used can get power from both electric supply &fuel complex structure having both electrical & mechanical drive drain free commercially	management of the energy sources Battery & engine size optimization
FCEV	Electric motor	Fuel cell	Very little or no emission High efficiency not dependent on electric supply of electricity High price Available commercially	cost of fuel cell easy way to produce fuel Availability of fueling facilities

2.2.2. Configurations

An electric vehicle, in contrast to its ICE partners, is very adaptable. these vehicles are power gotten from a battery and alternatively from ultra-capacitors. These batteries are charged from the electric framework. Additionally, a regenerative slowing mechanism can be used to charge the batteries when the EV is decelerating. Figure 2.2 expresses basic architecture in BEV.

- Battery the executive’s framework (BMS),

- Electric charger, which extricates energy from the electric organization to charge the batteries.
- Inverter or motor drive, which changes direct flow into rotating flow. It gives capacity to electric driving motor of the vehicle.
- Electric motor. which gives the mechanical force required by the vehicles.

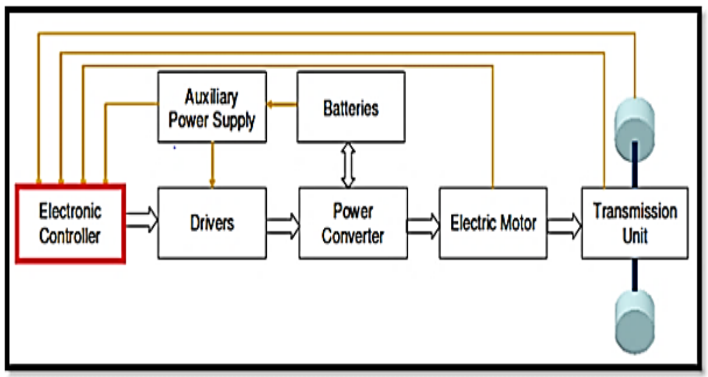

Figure 2.2 Battery electric vehicle basic architecture[9]

2.2.3. The Control Strategy for EV System

Here, controller is the core of an electric vehicle and it is the key for the acknowledgment of a superior electric vehicle with an ideal equilibrium of greatest speed, speed increase execution, and voyaging range per charge. The engine control framework signal, the speed increase pedal sign, the brake pedal sign, and signals of different parts are first gathered by the Vehicle Control Unit, which investigations the driver's expectation and makes comparing judgment. To arrange the development of different force segments and ensure ordinary driving of electric vehicles, the necessary engine yield force and different boundaries are determined. The vehicle is driven by motor and the energy is provided by the battery through a controlled force circuit. The engine is driven by the engine regulator and it moves the e-power into mechanical ability to drive the vehicle regulators are regularly delivered by enormous auto enterprises with cutting edge innovations and are principally utilized for complex four-wheel drive and wheel engine drive unadulterated electric vehicles. The vehicle control framework comprises of vehicle regulator, engine and engine regulator, power battery, power battery the executive’s framework (BMS), issue determination the board unit, gearbox, principal reducer, assistant framework, and different segments. The assistant framework incorporates directing engine and its regulator, cooling engine and its regulator, slowing mechanism, DC-DC converters and so forth The driver accomplishes the general control of the vehicle through the vehicle control system[10].

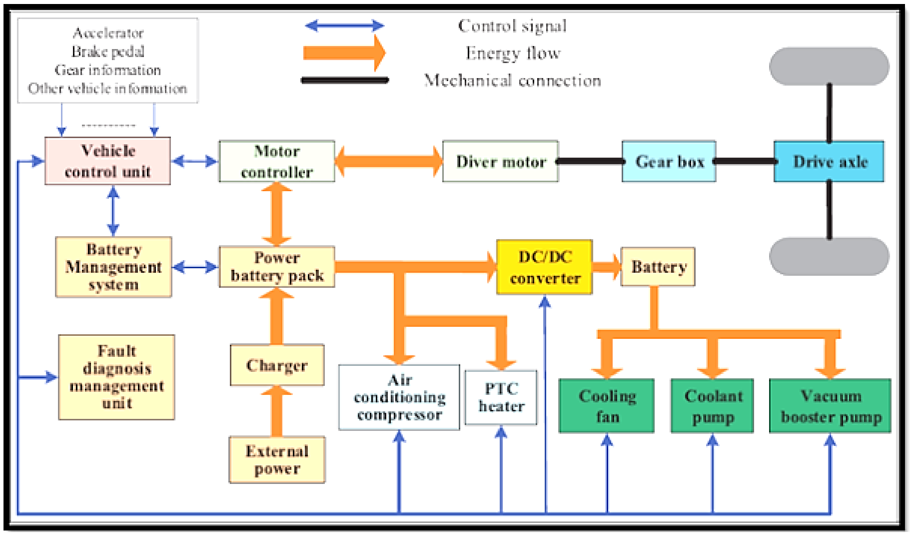

Figure 2.3 Structure of the control strategy for EV system[9]

The regulator gets the activity data from the driver, for example, the gas pedal, the brake pedal, and the shift switch signal. At that point the driver's expectation and the comparing activity are resolved dependent on the data. At the point when the vehicle is running, the vehicle yield force and the vehicle status are shipped off the engine control unit. At the point when the vehicle starts and stops, the high and low voltage power, which is provided by the outer related hardware, is controlled to turn on and off in succession. The beginning and running condition of the engine regulator and force the executive’s framework.

2.2.4. The Advantages of EV

Compared with common motor driving vehicles, EV has the accompanying advantages[10].

- Significant degree of effectiveness: the motor proficiency of present-day vehicles is about 38% while a definitive productivity is just 12% as a result of incessant slowing down, low speed driving and sign pausing. However, EV endures no loss of sits and 80% of the e-force can move from motor into vehicle movement. Moreover, it can recover power when braking.

- Low level of energy consumption: Fueled by batteries and super capacitors, unadulterated electric vehicle releases no waste gas.
- Low pace of clamor: The commotion and vibration of the auto relies upon the motor and the driving condition. Contrasted with motors, EV has many less vibration sources, no consuming methodology, no mechanical movements, just has clamors from air blower, cooling fan and transmission component. Subsequently its commotion level is a lot of lower than motor vehicles.
- Different energy assets accessible: Not limited by petrol asset, EV can gain e-power from public force framework. Hence any technique to gain e-force can apply to EV, for example, hydro power, atomic force, thermos power, wind power, underground warmth and sun-based power.
- Energy input by the energy asset blend instrument, All the new EV created lately have energy recovering framework, which can expand the ceaseless mileage by 10%-15%[11].

2.2.5. The Driving Character of Pure EV

In an EV the essential necessities of the EV to the driving control framework are as follows[12],

- High explicit force.
- Large scope of motor speeding, generally in 25%-100% most extreme speed.
- Sufficient beginning force to qualify the interest of quick beginning, speeding up, climbing and regular beginning/stop.
- Fast force reaction. The driving framework can handle the driving force and slowing down force rapidly.
- Good natural versatility.
- High pace of energy recovers in regenerative braking.
- Have great attributes of productivity. Increment the consistent driving distance in the wake of charging 1 time, for the most part ought to gain 85%-93% effectiveness in run of the mill circuit driving zone.

2.2.6. Regenerative braking in battery electric vehicle

Battery electric vehicles use the motor as a generator when using regenerative braking and operated as a generator during braking. Its output is supplied to electrical loads and it provides the braking effect. EV propulsion requires the motor drives offering four-quadrant characteristics for forward motoring, forward regeneration, backward motoring, and backward regeneration. The definition of 4 quadrants and thus the corresponding torque-speed characteristics are summarized in Table 2.2 Particularly, the forward regeneration is crucial to capture the braking energy which successively charges the EV battery, leading to increase the range per charge by over 10%. Figure 2.4 shows the schematic of PMBLDC motor drive where the input voltage is that the battery voltage, V dc, the input DC current I dc is bidirectional[13], the motor speed depends on the stator frequency, and its polarity is governed by the phase sequence. When the motor drive operates at Quadrant I for forward motoring, the torque and speed are positive that the input and output powers of the inverter are positive. Thus, the common input DC current to the inverter must be positive since the battery voltage is in fact positive. Because the motor speed is positive, the phase sequence of the stator terminals is positive, namely, A-B-C. When the motor drive operates at Quadrant IV for forward.

Table2. 2 Four-quadrant operations

Quadrant operation	Quadrant	Torque	Speed
Forward Motoring	I	Positive	Positive
Backward regeneration	II	Positive	Negative
Backward Motoring	III	Negative	Negative
Forward regeneration	IV	Negative	Positive

The speed is positive but the torque is negative so that the input and output powers of the inverter are negative. Thus, the average input DC current becomes negative so that the braking energy is converted for charging the battery. As the motor speed is still positive, the stator phase sequence is positive. The operations at Quadrants III and II are similar to that at Quadrants I and IV, respectively, except that the motor speed is negative and the corresponding stator phase sequence is negative, namely, A-C-B. The input DC current and stator AC phase sequence for four-quadrant operation of the PM BLDC motor drive is summarized in Table 2.2. [1]

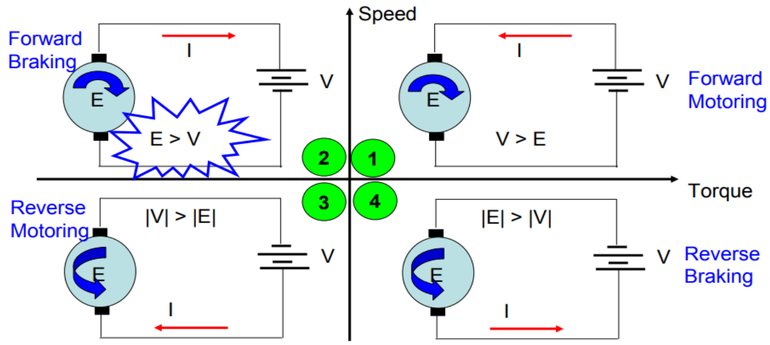

Figure 2. 4 four-quadrant operation of the PM BLDC motor drive[14]

For a BLDC motor to function in 2nd quadrant the value of the back emf created by the BLDC motor ought to be more prominent than the battery voltage (DC bus voltage) this guarantees that the movement of the current reverse whereas the motor still runs within the forward direction.

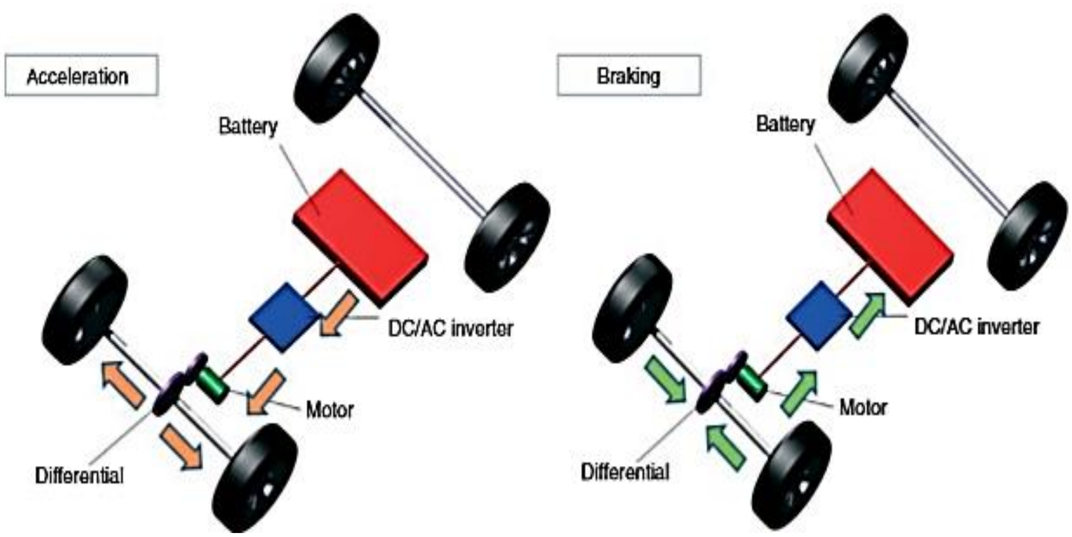

Figure 2. 5 Regenerative braking system of the pure electric vehicle.[15]

. Regenerative braking systems are categorized into two categories:

Category A: an electric regenerative braking framework which isn't portion of the benefit braking framework; and might be actuated by the quickening agent control and/or the equip impartial position

Category B: an electric regenerative braking framework which is portion of the benefit braking framework, and might have as it were one activating unit which in our case is the brake pedal. The pedal/torque characteristics of a system implementing both strategies are shown in figure 2.6

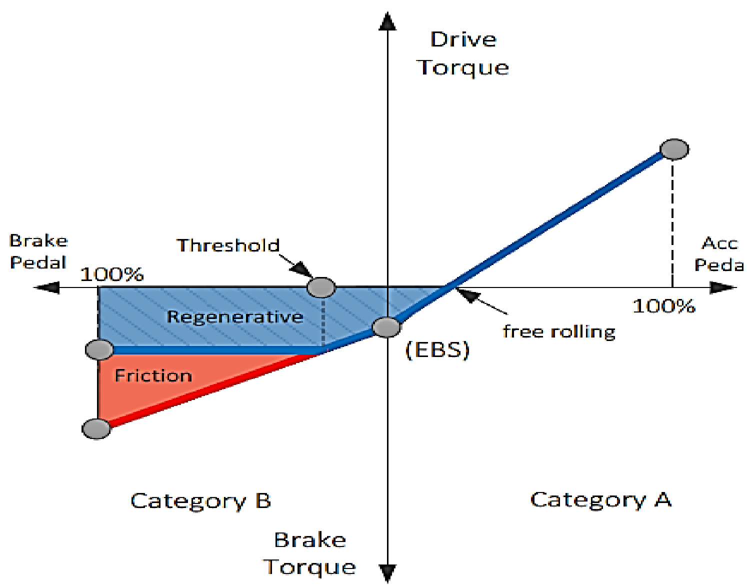

Figure 2. 6 Combined serial regenerative braking strategy (SBRS)[17]

As shown, when the quickening agent pedal is completely discharged the engine produces a negative braking torque causing the vehicle to decelerate. This braking torque upon discharge of the quickening agent can be set as Motor Brake Reenactment. It is additionally shown that in arrange to realize rolling (zero torque connected), the gas pedal ought to be squeezed to a certain position, called the free rolling or cruising point. The EBS seem to be set to and in this case, the line will go through the root meaning that no negative or positive torque will be connected when no pedal is connected and the vehicle is basically let to roll. The easiest way to realize a regenerative braking system is by simply adding up the deceleration caused by the motor and the braking system as done in serial regenerative braking systems[17].

2.2.6.1. Serial Regenerative Braking System (SRBS)

This type of system is easy to implement and very economical and is used when no big changes to the original braking system are to be made and no blending of electric and hydraulic braking is wanted. In such systems, the braking is purely electric at the beginning and after a given threshold (a defined pedal movement before the master cylinder is pressed). The amount of hydraulic braking torque that is applied is equal in magnitude to that not delivered electrically. This strategy is very good with low decelerations as in regular road driving where a large portion of the kinetic energy can be recovered. The biggest disadvantage is that the braking torque is speed dependent and is there-fore set either to a comfortable level or to a level that can be ensured at all rotational speeds.

2.2.6.2. Cooperative Regenerative Braking System (CRBS)

This type of system is also called parallel regenerative braking because it is capable of applying electric and hydraulic braking at the same time while being able to control the proportion of each separately and thus ensuring a total amount of needed braking torque independent of the motor rotational speed[17]. Figure 2.7 shows the relationship between the brake pedal and the generated braking torque.

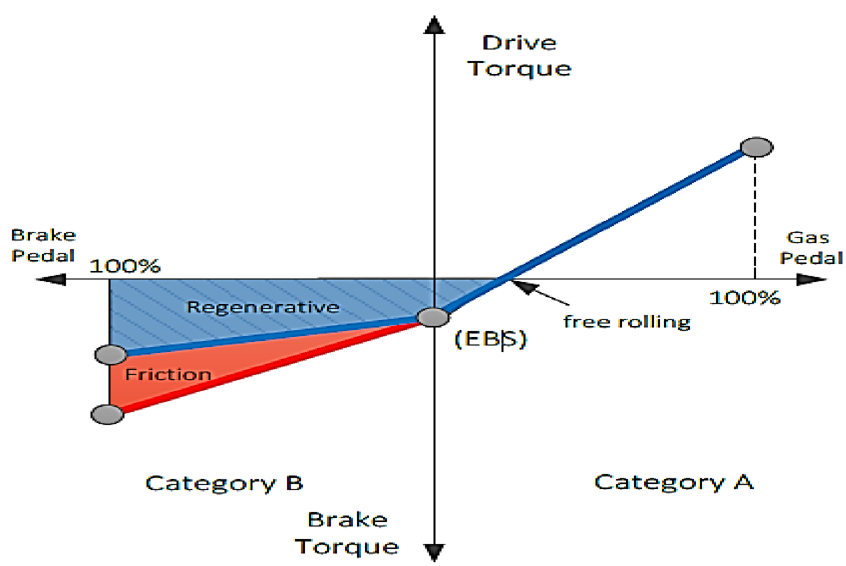

Figure 2. 7 Combined Cooperative Regenerative Braking Strategy (CRBS)[17]

2.3. Electric Motors

An electric motor is a field of electrical machine that changes over power into energy. Most electric motors work the connection between the motor's attractive field and electric flow in a very wire twisting to make power inside the force applied to the motor’s shaft. Electric motor will be controlled by direct flow (DC) sources for instance from batteries cars or rectifiers, or by substituting flow (AC) sources sort of a force matrix inverters or electrical generators.

Electric motors are divided in to three

- DC motor
- AC motor and
- others

2.3.1. Brushed DC Motors

In a brushed DC motor, the DC current going through the windings of the rotor creates an electromagnet. These rotor attractive shafts communicate with the posts of the fixed lasting magnet, called the stator, to make the rotor spin. After each half turn the rotor, to keep the motor turning, the rotor shafts should be flipped by switching the polarity of the flow in the winding. This exchanging of flow extremity is called commutation. Commutation occurs mechanically: Every half turn electrical contacts, called brushes, total a circuit to the next portion of the commutator on the rotor as it spins. Due to this physical contact, brushes wear out over time, keeping the motor from work in.

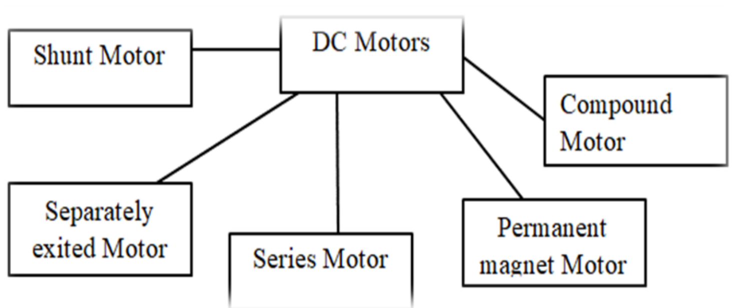

Figure 2. 8 classification of DC motors

Main important of Brushed DC motors

- High maintenance due to worn brushes
- Low efficiency
- Easy control (DC voltage

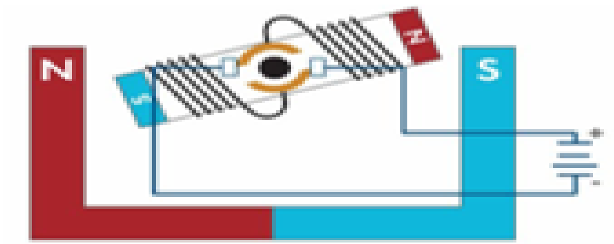

Figure 2. 9 Brushed DC motor

2.3.2. AC Motors

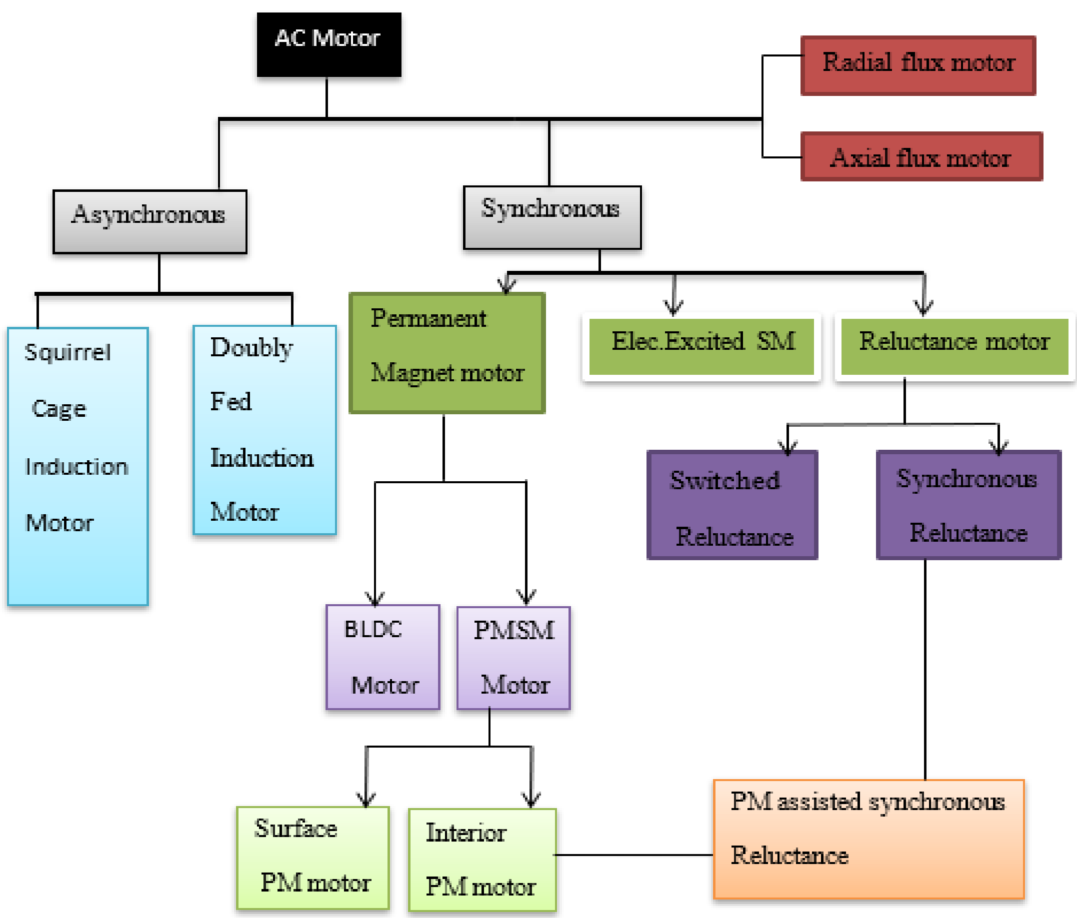

Figure 2. 10 Taxonomy of AC motors.

2.3.3. Permanent Magnet Synchronous Motor

They have truly reasonable properties for motor use; high remainder flux thickness and high strength against demagnetization. Since the field winding is supplanted by PMs, the PMSMs have low rotor dormancy and high force thickness. Further, since there is no auxiliary copper misfortune, the PMSMs have a higher efficiency than IMs. What's more, PMSMs are greater in fusing the hesitance force particularly in the field debilitating locale. Subsequently, PMSMs have a wide steady force speed range. Due to such benefits, PMSMs are prominently utilized in mechanical drives, home apparatuses, and electrical vehicles (EV).

2.3.4. Brushless DC Motor

BLDC motors donate higher advantage and require lower support which is the reason they have replaced brushed motors in a number of applications. Both sorts of motors work dependent on a comparable rule, in which the rotational movement is produced through the fascination and repugnance of attractive posts of perpetual and electromagnets. Nonetheless, the manner in which these motors are controlled is altogether different. BLDC require a mind-boggling regulator to change over a solitary DC capacity to three-stage voltage, while a brushed motor can be constrained by managing the DC voltage.

- Low maintenance
- High efficiency
- Complex control (DC to AC)

There are motors with different magnet arrangements where the stator may have various quantities of windings and the rotor may have different post combines as can be found in the accompanying figure 2.11.

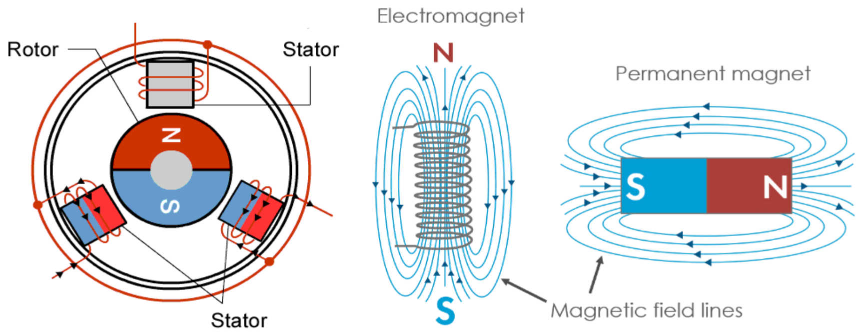

Figure 2. 11 BLDC motor and their magnetic arrangement

2.3.4.1. Permanent Magnetic BLDC Motor Drives

A PM motor force may be potentially designed with excessive energy density, excessive velocity, and excessive operation efficiency. This distinguished BLDC motor force is the maximum promising quality for EV and HEV applications.

The main advantage of a BLDC motor summarizes as the following:

- High efficiency: BLDC vehicles are the maximum green of all electric powered vehicles because of the usage of PMs for excitation
- Compactness: Rare-earth magnets has made it feasible to reap very excessive-flux densities in BLDC vehicles. Which makes feasible to reap excessive torques, flip permits one to make the motor small and light.
- Ease of manipulate: A BLDC motor manipulate variables are perform without difficulty reachable and regular all through the operation of the motor.
- Ease of cooling: the rotor of a BLDC motor does now no longer warmness up
- Low renovation, tremendous toughness, and reliability: The absence of brushes and mechanical commentators reduces the want for related normal renovation and reduces the threat of failure related to those elements.
- Low noise emissions.

BLDC motor drives are afflicted by a few negative aspects as follows:

- High Cost.

- Limited regular energy variety: A massive regular energy variety is vital to reaching excessive car efficiencies. The PM BLDC motor is incapable of reaching a maximum velocity more than two times the bottom velocity.
- Safety: Large rare-earth PMs are risky for the duration of the development of the motor due to the fact flying metal gadgets are drawn to them. There is likewise a threat with inside the case of car destroys if the wheel spins freely: the motor remains excited through its magnets, and excessive voltage is gift on the motor terminals, which could endanger passengers or rescuers.
- Magnet demagnetization: Magnets may be demagnetized through massive opposing magneto motive forces and excessive temperatures.

2.3.4.2. Comparing BLDC Motor to Other Motor Types

BLDC motors have many advantages with few disadvantages. The comparison between a BLDC motor and a brushed DC motor is summarizes in Table 2.3.

Table 2. 3 Comparing a BLDC motor to a brushed DC motor

Feature	BLDC Motor	Brushed DC Motor
Commutation	Electronic commutation Based on hall position sensor	Mechanical commutation.
Maintenance	Less due to absence of brushes.	Periodic maintenance is required.
Life	Longer	Shorter
Speed/Torque Characteristics	Flat – Enables operation at all speeds with rated load.	Moderately flat –At higher speeds, brush friction increases, thus reducing useful torque.
Efficiency	High – No voltage drops across brushes.	Moderate.
Output Power/ Frame Size	High – Reduced size due to superior thermal characteristics. Because BLDC has the windings on	Moderate/Low – The heat produced by the armature is dissipated in the air gap, thus increasing the temperature in

Output Power/ Frame Size	High – Reduced size due to superior thermal characteristics. Because BLDC has the windings on	Moderate/Low – The heat produced by the armature is dissipated in the air gap, thus increasing the temperature in
Control Requirements	A controller is always required to keep the motor running. The same controller can be used for variable speed control.	No controller is required for fixed speed; a controller is required only if variable speed is desired.

Electric motors are the heart of electric vehicle, which have different performance characteristics, based on that performance characteristics motor can select according to the vehicle specification to drive in safe and enough energy source ability as shown Table 2. 4

Table2. 4 Comparison of motors for electric vehicle selection

DC motor	BLDCM	PMSM	IM	SRM
efficiency less than 75%	High energy efficiency (greater than 95%), due to not have rotor winding and rotor copper loss	High energy efficiency 80%),	High energy efficiency (greater than 90%),	High energy efficiency (greater than 83%),
Low power density than SRM	High power density 1	Less power density than BLDC 2	Less power density than PMS (3)	Low power density
Low cost than others	High cost than other	Less cost than BLDC	Low cost than PMS	The 2nd low cost than others

2.3.4.3. Switching operation for Brushless DC Operation

There are two sorts of switching operations to drive this PM BLDC machine[16] .

- Two-phase 120∘ conduction scheme

Table2. 5 Hall sensor and motor phase in 120∘ operation.

	Hall sensor			Motor phase		
step	HA	HB	HC	A	B	C
1	1	1	0	OFF	+	-
2	1	0	0	+	OFF	-
3	1	0	1	+	_	OFF
4	0	0	1	OFF	-	+
5	0	1	1	-	OFF	+
6	0	1	0	-	+	OFF

Within the two-phase 120∘ conduction operation, at any instant, only two phases are conducted with the conduction interval of 120∘ while the remaining phase is non-conducted as depicted in Figure 2.12. The corresponding switching sequence is summarized in Table 2.4

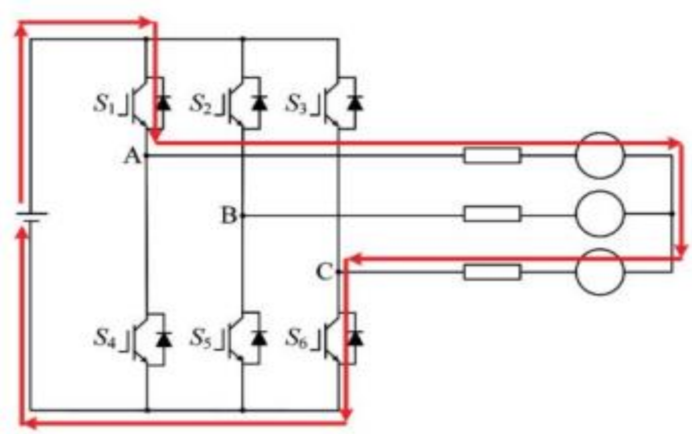

Figure 2. 12 Current flow under two-phase 120∘ conduction opration[17]

Table2. 6 Switching sequence under two-phase 120∘ conduction operation

Interval (∘)	Device on	Phases A, B, C
0-60	S1, S6	+,0, -
60-120	S2, S6	0, +, -
120-180	S2, S4	-, +,0
180-240	S3, S4	-,0, +
240-300	S3, S5	0, -, +
300-360	S1, S5	+, -,0

For normal operation, the phase current waveform is near rectangular in shape and easily reaches this demand as shown in Figure 2.13.

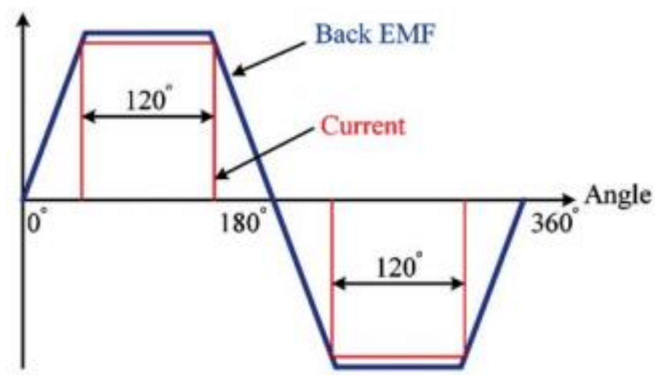

Figure 2. 13 Phase back EMF and current waveforms under two-phase 120∘ conduction opration.

- Three-phase 180∘ conduction scheme.

Within the three-phase 180∘ conduction operation, all three phases are conducted with the conduction interval of 180∘ as depicted in Figure 2.13. The corresponding switching sequence is summarized in Table 2.7. For normal operation, the phase current waveform is near quasi-square in shape and easily reaches the demanded current as shown Figure 2.14 below.

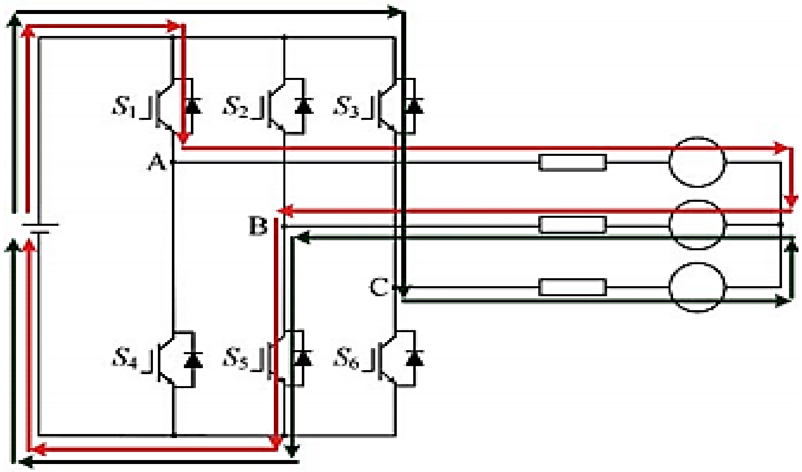

Figure 2. 14 circuit diagram of Current flow under three-phase 180∘

Table2. 7 Switching sequence under three-phase 180∘ conduction operation[17]

Interval (∘)	Device on	Phases A, B, C
0-60	S1, S5, S3	+,-,+
60-120	S1, S5, S6	0, -, -
120-180	S1, S2, S6	+,+,-
180-240	S4, S2, S6	-,+,-
240-300	S4, S2, S3	-,+,+
300-360	S4, S5,53	-,-,+

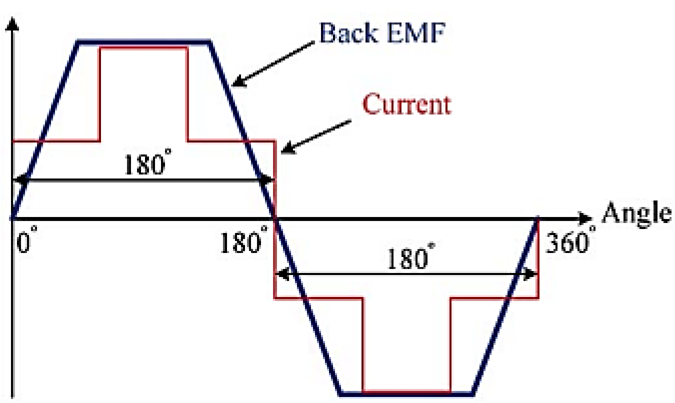

Figure 2. 15 Phase back EMF and current waveforms under three-phase 180∘ [17]

Table2. 8 Comparison between 120◦ and 180◦ switching operation

Switching operation 120◦ conduction	Switching operation 180◦ conduction
Advantage torque capability for identical phase current	only switching one device on or off
Maximize the developed torque and efficiency	minimize the switching loss and chance of contact
more preferable	torque ripple is larger
	phase current is fed where the rear EMF isn't constant

2.3.4.4. Three phase inverter working principle

To control the phases during six-step commutation, a three-phase inverter is important to convert the DC voltage to the three phases current.

The switch sequence indicated that positive current turned on the high side and negative current turned on the low side.

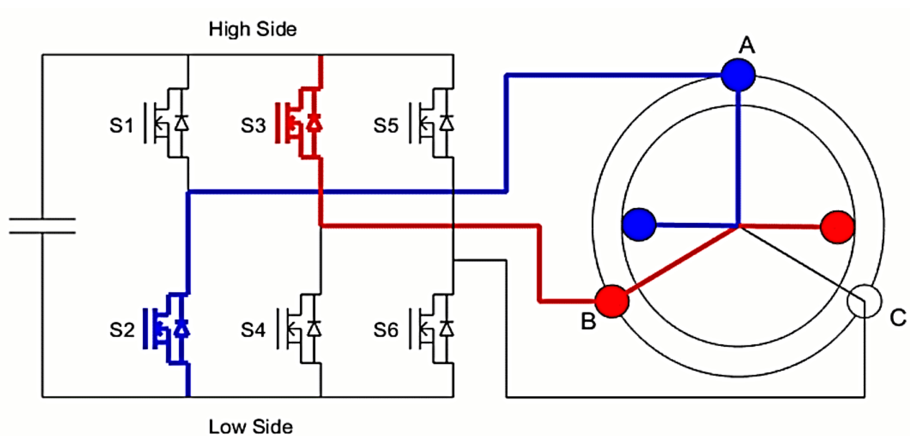

Figure 2. 16 Three phase inverter working principle

Figure 2.16 describes the rotor is at an angle between 60 and 120 degrees to the stator magnetic field, the three-phase inverter keeps the motor rotating at a constant speed. Varying motor speed can be achieved by adjusting the applied voltage. Another way of controlling the motor speed without varying the source voltage is pulse-width modulation, or PWM.

2.4. Electric Vehicle Batteries

An electric-vehicle battery (EVB) moreover to the traction battery specialty frameworks utilized for mechanical (or recreational) vehicles, are the batteries need to control the electrical motors of battery electric vehicle (BEVs). Batteries for electric vehicles are characterized by their moderately high power-to-weight ratio, particular energy and energy density; smaller, lower battery decrease the load of the vehicle and improve its performance. Compared to fluid fuels, most current battery innovations have much lower particular energy, and this frequently impacts the maximal all-electric range of the vehicles. However, metal-air batteries have tall particular energy since the cathode is given by the encircling oxygen inside the air.

2.4.1. Types of Electric Battery

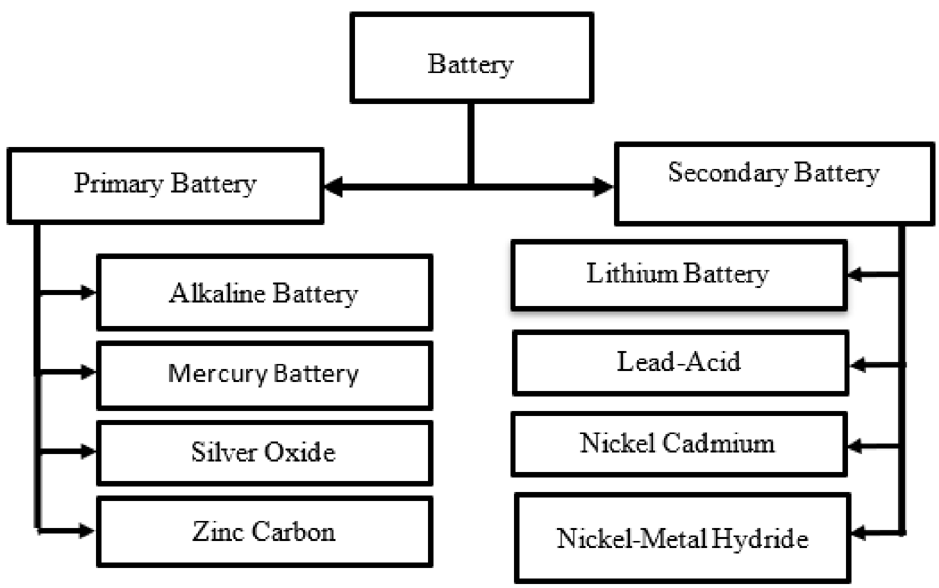

Figure 2. 17 Types of Electric Batter

2.4.2. Comparison of Electric batteries

Table 2. 9 Comparison of Electric batteries[18]

No.	Types of Battery	Advantage	Disadvantage
1	Lithium-ion Battery	High energy density High power rate cycle life Longer run time High efficiency No loss of amp hours	Expensive Technology not properly developed
2	Lead-Acid	High power density Medium efficiency Loss of 15-amp hours Reliable and cheap	Low energy density High maintenance Vary large and old type Bulky
3	Nickel Cadmium	Good life cycle Available in different size	Low output voltage Expensive and Toxic
4	Nickel-Metal Hydride	High-capacity energy density Same size	More complex charging algorithm needed High self-discharging Low power rate

In general, the comparison performance of battery for EV propulsion can be summarized as shown in figure 2.18 based on battery performance characteristics of each maximum of five points. Lithium-ion batteries have great performance parameters than other types of batteries for EV. It has higher energy density, longer era and better power density than most other practical batteries. The Complicating factors include safety, durability, thermal breakdown and price. Li-ion batteries should be used within safe temperature and voltage ranges so as to work safely and efficiently as shown from Figure 2.18 below [18].

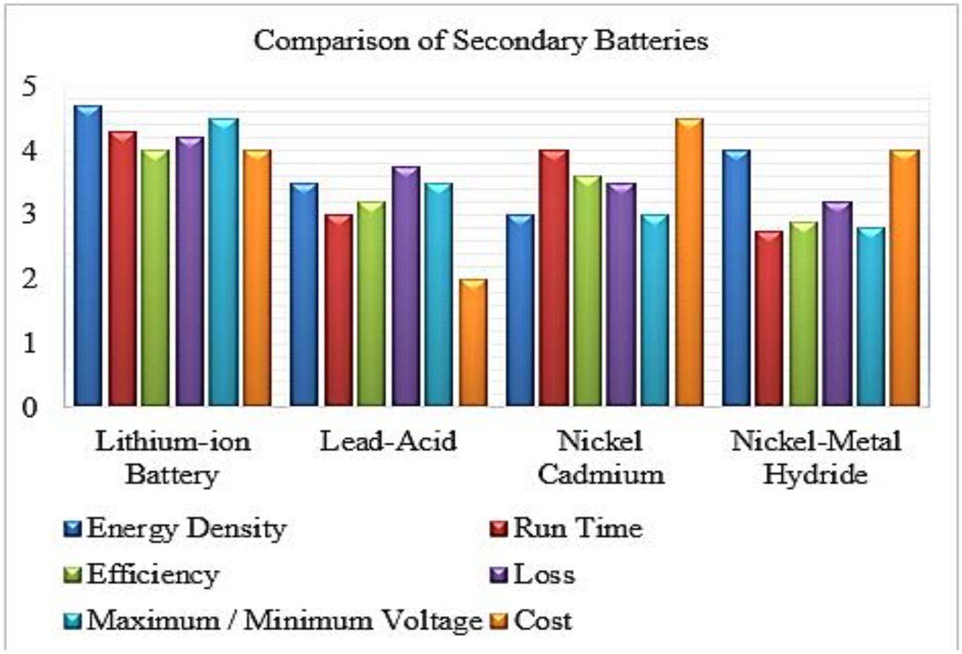

Figure 2. 18 Comparison of Secondary Batteries

From Figure 2.18 the parameters are measured with Energy density(J/m^3), Efficiency (%), Maximum/minimum voltage (V), Run time (second), loss (L) and cost (kWh)

2.5. Bidirectional DC-DC Converter

A bidirectional buck-boost convertor is different from a unidirectional DC/DC Converter it utilizes MOSFET or IGBT to switch the state of the current rather than all the diodes [7]. The size of the voltage and current as well as the arrangement of the energy capacity things, the bi-directional DC-DC converter can either operate as a Buck converter by stepping down the next voltage to a lower voltage or as a Boost converter by stepping up from a lower voltage to the higher voltage. Undoubtedly, diodes do not permit current to flow in both directions, but with MOSFET the period of each position can be effectively controlled. The kinetic energy is wasted as heat energy in previous method while this energy includes the transformation of kinetic energy into electric energy which is purified and stored in a chargeable battery in car applications. most DC/DC converters have to be trade control between two voltage sources [24]. To achieve this power, transfer the current must be able to go through the circuit in both directions. There are a lot of for this kind of converters, because the use of a battery implies the capacity of charging and discharging so the use of a bidirectional converter allows avoiding a complex system of twin circuits to accomplish the charge and the discharge of the battery.

2.6. Particle swarm optimization algorithm

Particle Swarm Optimization (PSO) may be a population-based globalized look calculation that employments the standards of the social behavior of swarms. PSO produces superior comes about in complicated and multi-peak issues. The PSO calculation is exceptionally quick, straightforward and simple to get it and execute. It moreover has few parameters to alter. PSO finds the finest esteem with interaction of molecule, but when the look space is tall its merging speed gets to be exceptionally moderate close worldwide ideal. It moreover appears destitute quality comes about when it bargains with huge and complex information set. As previously mentioned, a few PSO variations have been created to overcome this issue[22].

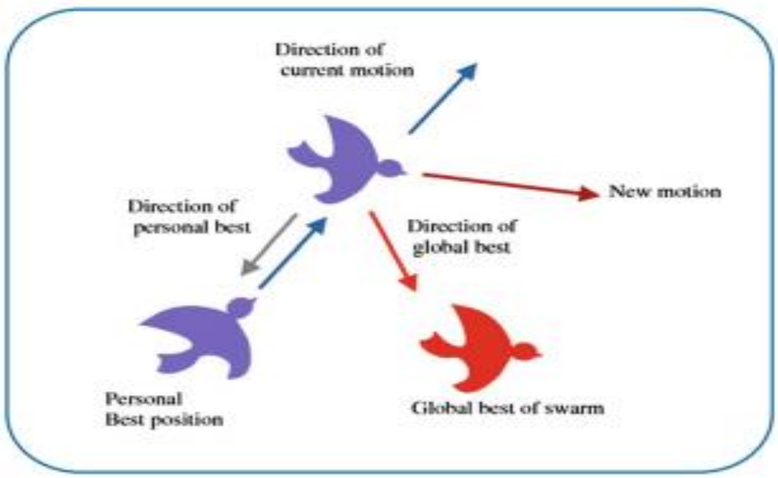

Figure 2. 19 Representation of upgrading the speed of a particle[22]

2.7. Related Works

The global interest in reducing fuel consumption has led to the emergence of different types of electric vehicles like battery electric vehicle. The battery plays an important role in providing the power required by the driver. The development of greener and fuel-efficient cars can be achieved in two different ways: the development of more advanced car hardware and better control techniques. Since the latter is more profitable, more researchers pay attention to it and some papers are presented in this research.

A study on Regenerative braking system with MATLAB simulation was proposed to study regenerative braking used in electric vehicles and to prepare a mathematical model of the system with the help of MATLAB/SIMULINK [4]. This study shows that the BLDC motor is the suitable motor for performing regenerative braking operation. Additionally, the paper used a PID controller to implement the PWM to the inverter that can maintain constant braking torque. An adaptive technique is also used to adopt PID parameters. Due to this adaptive technique, the system response is very slow. This paper did not mention anything about the current which is the other drawback of the study.

The authors in [23] proposed a novel regenerative braking scheme for electric vehicle driven by brushless dc motor. This paper used fuzzy logic to utilize regenerative braking energy effectively. The controller used in this study gives a smooth brake but the response is very slow due to large number of fuzzy rules.

Design of a controller for regenerative braking using BLDC motor applicable for EV was presented to design a PID with fuzzy logic controller that produces significant improvement in control performance [24]. In this paper, the PID gains are tuned by fuzzy controller. Hence, the system response is to slow because of the fuzzy rules. To overcome this issue, PSO is utilized for tuning the PID controller and gives fast response. This thesis solves the above problems by designing a PSO based PID speed control of BLDC motor drive with regenerative breaking for EV application. Furthermore, the braking energy, energy loss in figure 4.13 the result shows it lost 0.05% within 0 to 0.5sec. during regenerative braking from

CHAPTER THREE

METHODOLOGY

3.1. Introduction

This chapter deals with data collection mechanism and analysis, mathematical modeling of the vehicle dynamics and BLDC motor, and design of speed control and inverter switches techniques for the BLDC motor drive. PID –PSO control technique is applied for speed control of the motor. The artificial intelligence based linear PID controller tuning methods are performed for speed control of BLDC motor. Hysteresis current regulator is developed to limit the flowing current of the motor. Then modeling of the overall BLDC motor drive is performed. Finally, the system is simulated by using MATLAB/2021a software both in Simulink and script.

3.2. Materials

In this research work, software such as MATLAB/2021a, Microsoft office 2019, and Math Type 6.0 equation are used. MATLAB is the computing software which consists of technical toolboxes and Simulink. Microsoft office is used for editing the thesis documentation. Math Type 6.0 is used for writing mathematical formulas and equations in Microsoft offices word and PowerPoint presentation tools.

3.3. Methods

The method utilized in this thesis to accomplish the specified task is shown in Figure 3.1. The closely related papers and literatures are reviewed. Then the required data used throughout this research are collected and analyzed. BLDCM has been widely used in EV because it's more efficient and is more easily controllable than other AC motors [12]. So, regenerative braking of EV that uses power from battery supported BLDCM is discussed during this research. Electric vehicle BLDC motor specifications have taken from the manufacturing company and a few of the opposite specifications taken from literatures. The collected data is analyzed mathematically and graphically for developing system modeling.

The dynamics modeling and therefore the maximum power requirement of BEV is analyzed. The BLDC motor speed control drive is intended with inverter commutation techniques supported the BEV and also the motor controller result, the BEV speed is analyzed in km/h with the battery state of charge and therefore the model of braking current is established, on the idea of which auto disturbances rejection controller is meant to appreciate good control effects of regenerative braking. The proposed modeling and simulation results of the system is compared with different AI based control algorithms for speed and current control. Different three phase inverter commutation techniques are applied and compared throughout the work. The diagram in Figure 3.1 summarizes the tactic followed throughout the research work.

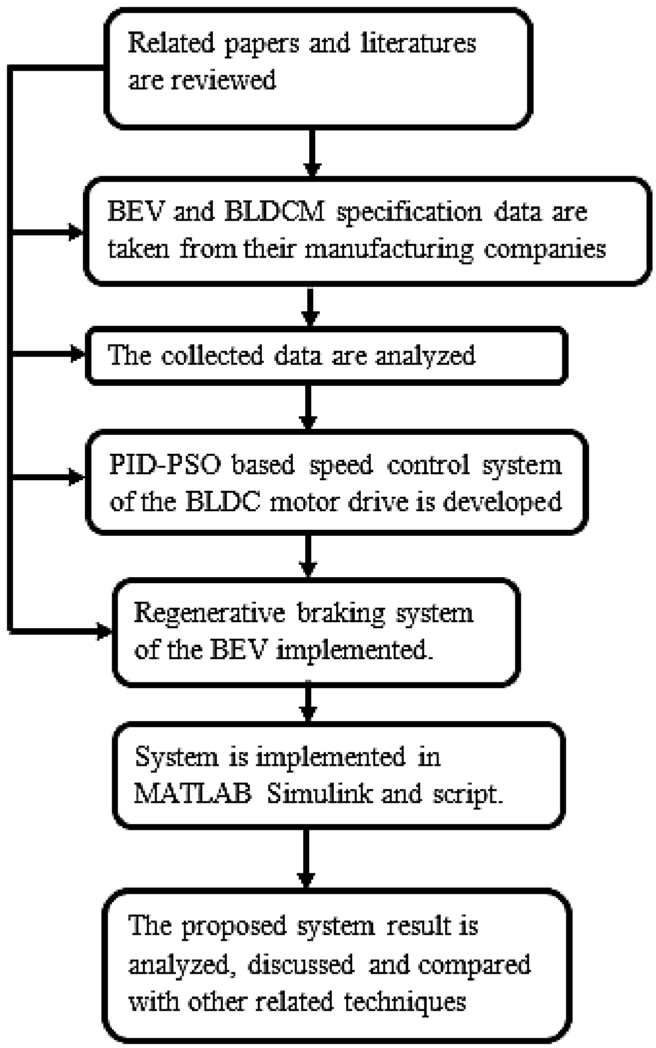

Figure 3. 1 Block diagram of research methodology

3.4. Analysis of electric vehicle system development and dynamics modeling

The Following are the key components in Electric vehicle:

- Battery Charger
- Battery
- Motor Controller
- Motor
- DC-DC Converter
- Vehicle Computer and Electronics

The electric vehicle is the easiest in structure. The key components are the driving parts. Figure3.2 shows the configuration.

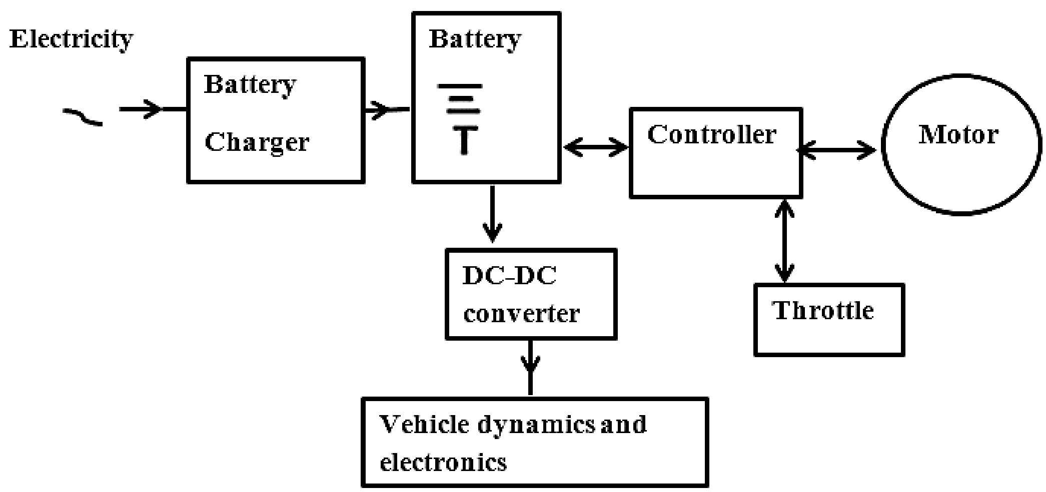

Figure 3.2 The key components of Electric Vehicle

The battery is that the main energy storage. The battery voltage is DC and current (I) is converted into switched-mode signal through control electronic controller to drive the motor. The opposite electronic components during a vehicle are often supplied to the battery through DC-DC converter that can either boost up or step down the voltage supported the dynamic vehicle requirement. The vehicle dynamics model is critical to be designed to develop a regenerative braking controller. Because the main research during this paper is breaking performance of electrical vehicles, only the longitudinal motion is taken into account in vehicle dynamics model. Furthermore, the direct braking condition is assumed and no stable effect is taken into account as far as Table 3.1 shows the typical values of tractive effort coefficients on various roads. The traction coefficient is highly passionate about the roughness, the contacting area, and therefore the frictional force pulling or pushing a vehicle's mass.

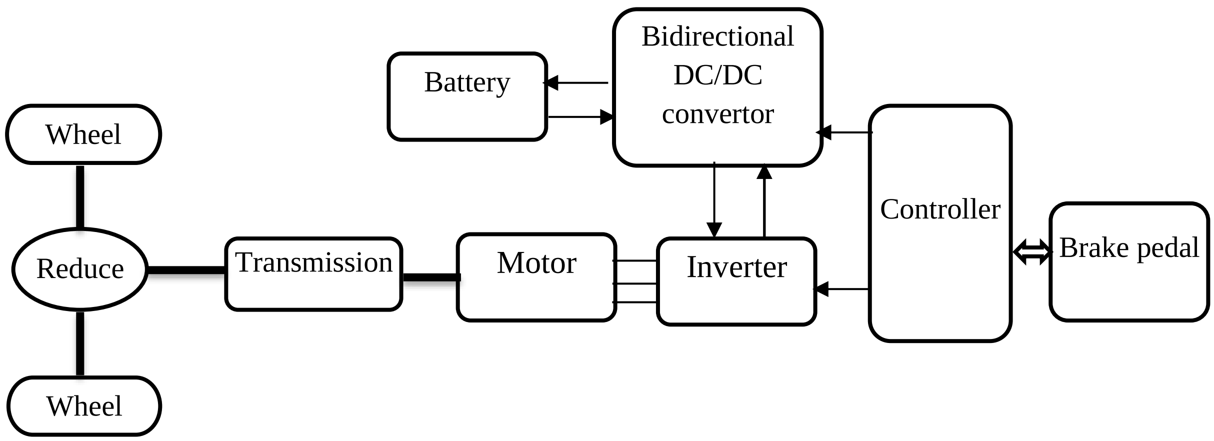

Figure 3.3 BEV Regenerative braking block diagram

From Figure 3.3, when the driver apply brake pedal the motor act as a generator that changes mechanical energy into electrical energy and this energy is stored in battery. Since the battery uses a DC voltage, the bidirectional DC/DC converter is used to convert the inverter AC voltage to DC voltage during braking time. When the stored energy is required by the vehicle, the bidirectional DC/DC converter convert the DC voltage from the battery to AC voltage that is given to the inverter.

Table 3.1 Average Values of Tractive Effort Coefficient on Various Roads [8]

surface	Peak Values, μp	Sliding Values, μ
Asphalt and concrete (dry)	0.8–0.9	0.75
Concrete (wet)	0.8	0.7
Asphalt (wet)	0.5–0.7	0.45–0.6
Grave	0.6	0.55
Earth road (dry)	0.68	0.65
Earth road (wet)	0.55	0.4–0.5
Snow (hard packed)	0.2	0.15
Ice	0.1	0.07

The behavior of a vehicle system and its dynamics involves a balance among the several acting forces.

Table 3.2 The 2019 BMW i3 42 kWh electric vehicle specifications[19]

Specification	Values
Vehicle weight at full, average (Mv)	1345kg
vehicle length (L)	4.011m
vehicle height	1.598m
the wind speed (Vwind)	20m/s
Frontal area (Af)	2.83kg/m2
Maximum running Vehicle speed (Vx)	41.67m/s or 150Km/h
Wheel base	2.57m
Length of vehicle from center to front (La)	1.572m
Length of vehicle from center to rear (Lb.)	1.575m
Height of vehicle from ground to center (hg)	0.57m
Aerodynamic drag coefficient (Cd)	0.3
Wheel rolling radius(rd.)	0.3m
the angle of inclination of the road (β)	0~0.174 (rad) or 9.97degree
the acceleration due to gravity (g)	9.819 (m/s^2)
the air mass density (ρ)	(1.2 kg/m^3)
the rolling resistance coefficient (μr)	0.01
coefficient of longitudinal friction(μ)	0.4~1
Maximum torque	250Nm
Rated speed	4800rpm
the moment of inertia of the wheel (Jw)	0.5 (kg/m2)
Average starting Acceleration(av)	0.95 m/s^2
Inertia of the vehicle	1.7
Rated torque	149Nm
Gear ratio	9.665:1

These forces are categorized into tractive (Ft) and road-load forces. The tractive effort appears within the contacting area between the driving wheel and so the level and moves the vehicle forward. It’s produced by the torque powerhouse and transferred through transmission and final drive to the wheels. While the vehicle is moving, there are road-load resistances that attempt to stop its movement. These road-load forces include rolling resistance of the tires, the aerodynamic force, frictional force of the slope and force due to vehicle inertia. in line with the Newton's second law, Equation (3.1) indicates that speed and acceleration rely on tractive effort, road-load force, and on the weight of the vehicle.

3.4.1. Vehicle Resistance Forces

During driving, resistance forces act on the vehicles. These resistance forces;

- Aerodynamic Resistance Force.
- Tire Rolling Resistance Force.
- Gradient Resistance Force.
- Inertia Resistance. Wind Resistance Force.

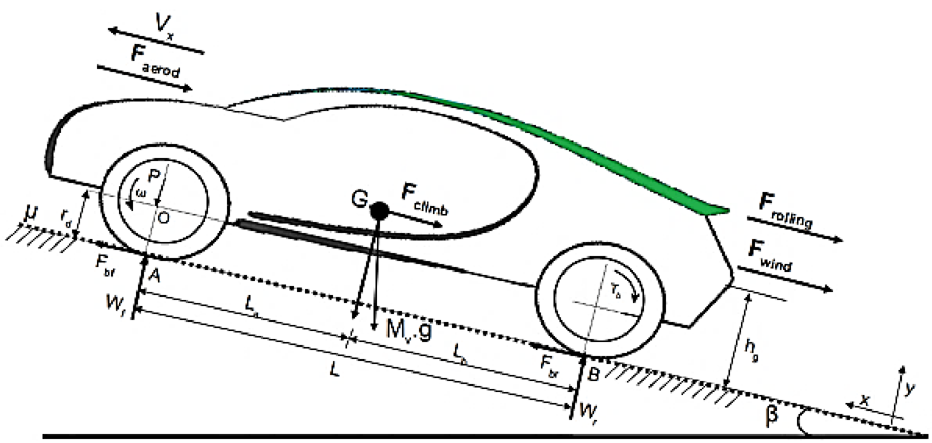

Figure 3.4 Electric Vehicle Dynamics[20]

3.4.1.1. Aerodynamic Drag Force

$$Faerod = \frac{1}{2} * \rho * Af * Cd * (Vx - Vw)^2 \left[N\right] \quad (3.1)$$

$$Faerod = 0.5*1.2*2.38*0.3*469.5889 = 201N$$

$$Paerod = Faerod*(Vx - Vwin) = 201N*21.67m/s = 4.359kw$$

Where, $Faerod$ = total aerodynamic resistance in N, Cd= the aerodynamic drag coefficient Af = the frontal area in m^2, Vw = wind speed in m/s, ρ = the air mass density in kg/m^3, Vx = the vehicle speed in m/s

3.4.1.2. Rolling Resistance Force

$$F_{rolling} = P * \mu_r = M_v * g * \mu_r * \cos(\beta)[N]$$
$$F_{rolling} = 1345 * 9.8 * 0.01 * \cos(9.97) = 129.9N \qquad 3.2$$
$$P_{rolling} = F_{rolling} * Vx = 129.9N * 41.67m/s = 5.41kw$$

Rolling resistance force ($F_{rolling}$) is the tangential force of normal force (P) on tires and the rolling resistance coefficient (μr).

3.4.1.3. Gradient Resistance Force

The gradient resistance or the hill-climbing resistance force (F_{climb}) is dependent on the weight of the EV and the angle of inclination β of EV is exposed.

$$F_{climb} = Mv * g * \sin(b) \quad [N] \qquad (3.3)$$
$$F_{climb} = 1345*9.8*\sin(9.97) = 2,282.05N$$
$$P_{climb} = F_{climb} * Vx = 2282.05N * 20.8m/s = 47.46kw$$

3.4.1.4. Acceleration Resistance Force

The linear acceleration force ($Facc$) is based on the mass of the vehicle (Mv), acceleration/deceleration of the vehicle (αv), and the vehicle speed (Vx) expressed as following:

$$F_{acc} = Mv * av = Mv * \frac{\delta Vx}{\delta t} \quad [N] \qquad (3.4)$$
$$F_{acc} = 1345 * 0.95 = 1277.75N$$
$$P_{acc} = F_{acc} * Vx = 1277.75 * 41.67m/s = 53.24kw$$

3.4.1.5 Wind Resistance Force

$$F_{wind} = C_w * A_f * V_{win}^2 [N]$$
$$F_{wind} = 0.299 * 2.38 * 400 = 284.6 \qquad (3.5)$$
$$P_{wind} = F_{wind} * Vx = 284.6 * 20.8m/s = 5.9kw$$

C_W is coefficient of wind resistance which is different for passenger cars (0.299), small trucks (0.43) and big truck. Based on all these equations the resultant force produces a counteractive torque to the driving motor. The total acting force is given by

$$F_{total} = F_{aerod} + F_{rolling} + \mathrm{F_{climb}} + \mathrm{F_{acc}} + \mathrm{F_{wind}}$$

$$F_{total} = 201N + 129.9N + 2282.05\mathrm{N} + 1277.75N + 284.6\mathrm{N} = 4175.3\mathrm{N} \tag{3.6}$$

$$P_{total}(\max) = P_{aerod} + P_{rolling} + P_{\mathrm{climb}} + \mathrm{P_{acc}} + \mathrm{P_{wind}}$$

$$P_{total}(\max) = 4.359\mathrm{kw} + 5.41kw + 47.46\mathrm{kw} + 53.24\mathrm{kw} + 5.9kw = 116.4kw$$

The total motive force with each component of the vehicle is shown in Figure 3.5. In this Figure 3.4 the vehicle is assumed to move up a hill with constant speed of 60Km/hr and the velocity of the air is also assumed to 20

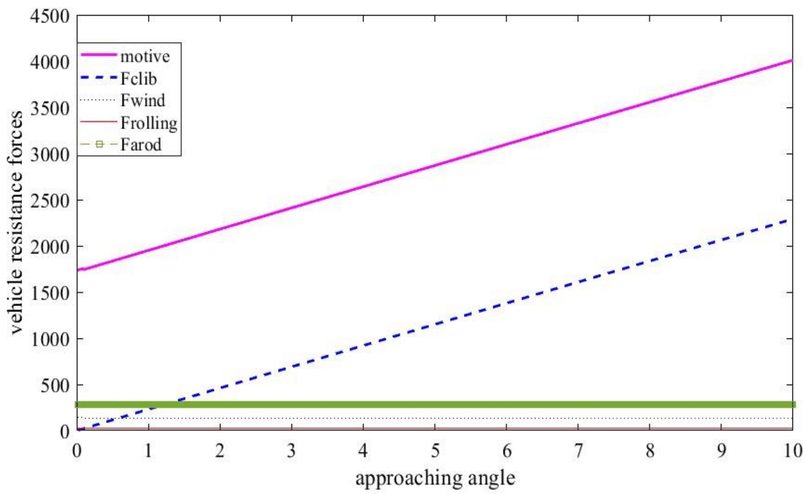

Figure 3.5 Motive force versus approaching angle of the vehicle

The BLDC motor with output power rating of 116.4kW should not be selected. [3] The losses due to transmission of power to the wheel must be included. Therefore, the mechanical power output required to move the vehicle is given by equation below:

$$\mathrm{M_{total(max)}} = \frac{\mathrm{P_{total(max)}}}{\eta_{\text{transmission gear syasem}}} \tag{3.7}$$

$$= \frac{116.4\mathrm{KW}}{0.93} \approx 125\mathrm{kW}$$

Equation (3.7) shows the total driving power of the motor for the propulsion of the meter. Based on this result, the motor rated specifications are selected as shown in Table 3.2.

3.5. Traction Motor Specification

According to the maximum power of the electric vehicle some of the BLDC motor specifications are taken from the manufacturing company and the others are taken from literature. The torque and back EMF constants are determined by the following derivations from the motor two phase equations [2]. The rated power of the motor is described by the product of the motor current and the back EMF for considering two phases.

$$\text{Power}_{rated} = 2E_m I_m \tag{3.8}$$

from Equation (3.8),

$$E_m = \frac{\text{Power}_{\text{rated}}}{2 * I_m}$$

$$E_m = \frac{75Kw}{2*120A} = 312.5V \tag{3.9}$$

Hence, the back EMF and speed of the motor are directly proportional to other

$$\text{EMF constant}(K_b) = \frac{E_m}{\omega_{\text{rated}}} = \frac{312.5V}{4800\text{rpm}} = 0.62201\left(\frac{V}{\text{rad/sec}}\right) \tag{3.10}$$

If two phase operating system of BLDCM is considered $K_b = 2\times 0.62201 = 1.24402$. Then the torque constant of the motor is calculated by

$$K_t = \frac{2 * E_{m(\text{rated})}}{\omega_{\text{rated}}} = \frac{2\times 312.5}{502.4\,\text{rad/sec}} = 1.24402 \tag{3.11}$$

$$\text{Torque}_{\text{rated}} = K_t I_{m(\text{rated})} = \frac{2 * E_{m(\text{rated})} * I_{m(\text{rated})}}{\omega_{\text{rated}}}$$

$$\text{Torque}_{\text{rated}} = K_t I_{m(\text{rated})} = 1.24402\times 120A = 149N \tag{3.12}$$

3.5.1. The Effect of Vehicle Speed on the Power Requirement

The relationship between the speed and driving power of the BEV is analyzed and plotted as shown in Figure 3.5. This shows that the vehicle power consumption and speed in km/hr have a linear relationship. As the speed of vehicle increases, its power consumption also increases [3]

[4]. The vehicle can move at the speed of 150km/hr. with a power consumption of 75kW. This relation fulfills with the identified maximum power requirement [2].

3.5.2. Motor Rated Power and Peak Power Matching

The selection of rated speed, torque, and power of the BLDC motor should conform to the requirements of the torque versus speed characteristic curve [52]. When the vehicle starts, the motor speed is low and works in constant torque state, as long as the speed is higher than the rated speed, it works in constant power state [53]. The rated torque and power of the 4800rpm base speed electric vehicle BLDC motor have a value of 149.2Nm and 75kW respectively as shown in Figure 3.6.

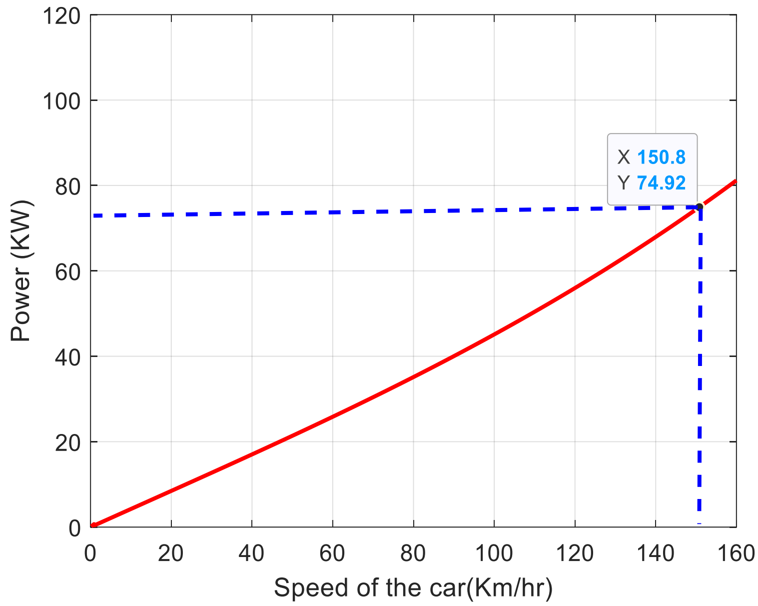

Figure 3.6 driving power vs speed of the electric vehicle

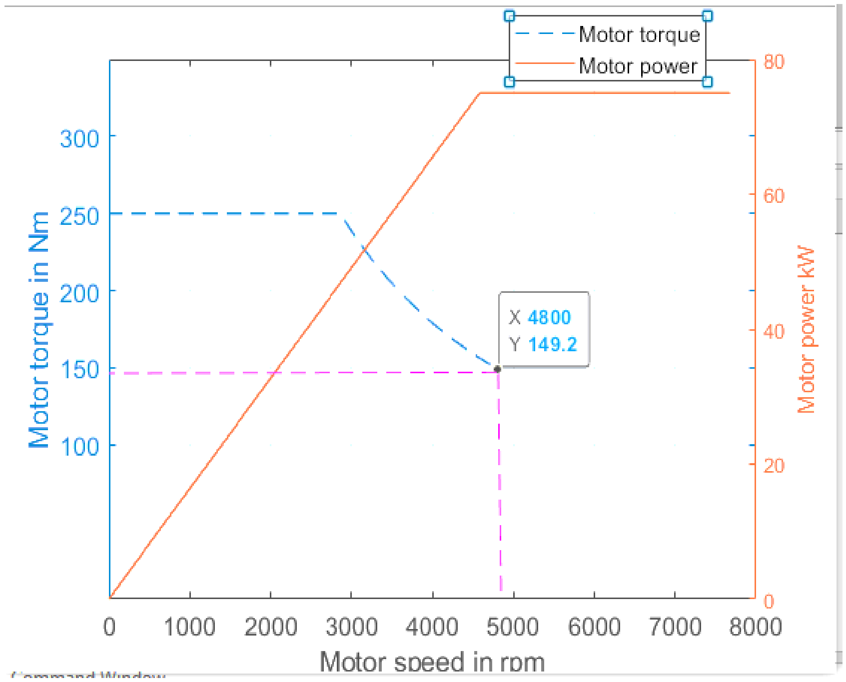

Figure 3.7 Torque versus speed characteristics of the BLDC motor

3.5.3. The Effect of Gradient Angle on the Power and Speed of Vehicle

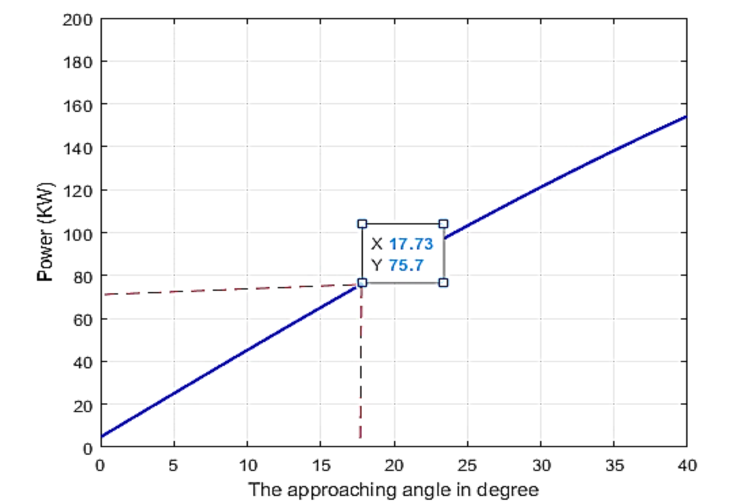

Figure 3.8 Driving power vs approaching angle of the vehicle

Table 3.3 Parameter's specification of BLDC motor used in this thesis [34]

Parameter name	Parameter value
voltage	480V (DC)
Maximum power	125kw
Rated power	75Kw
Rated speed	4800RPM
Motor connection	3-phase star connection
	(Six step commutation every 60 degree)
Rated current	212A
Control input rated voltage	352V
No. of poles (p)	4
Efficiency of the maximum power motor	0.93%
Efficiency of the rated power motor	95.7%
R (Phase stator resistance)	1.6 Ω
λp (The amplitude of flux linkage) Turns	0.105 Wb.
L (Self-inductance)	2mH
M (Mutual inductance)	0.5
Power factor	0.85
(L– M)	1.5 mH
B (Viscous coefficient)	0.001N.m. s
J (Moment of Inertia) Motor connection	1.42 * 10-4 Kg.m2
T (Full Load torque)	4 N.m
Torque constant	1.24402N-m/A
Back EMF constant	0.62201VS/rad

3.5.4. Electric Battery Specification

The proposed system equations considered for the battery are as follow

Table 3.4 Parameter specifications of Lithium-ion battery[21]

Parameter	values
Cell type	Lithium-ion
Total battery power pack	37.9KWh (42.2KWh gross)
Rated DC power supply	352V
Capacity	120Ah
Mass	4.5kg
Nominal voltage	5.2v
Energy density	155 Wh/kg
Operating temperature	-20°C to 55°C
Energy	540Wh

3.6. Wheel Dynamics

Figure 3.8 appears the principle of braking force variation between front and raise wheels, which happens when brake operations are performed whereas the vehicle is running on a level street. The vehicle braking operation depends on the vehicle mass (Mv) and acceleration/deceleration of the vehicle (a_v). The relationship between the vehicle braking driving force (Fv), the front wheel braking force (Fbf), and the raise wheel braking force (Fbr) can be represented as:

$$Fv = Mv * a_v = Fbf + Fbr \quad [N]$$
$$Fv = 1345 * 0.95 = 1,277.75 \quad [N] \tag{3.13}$$

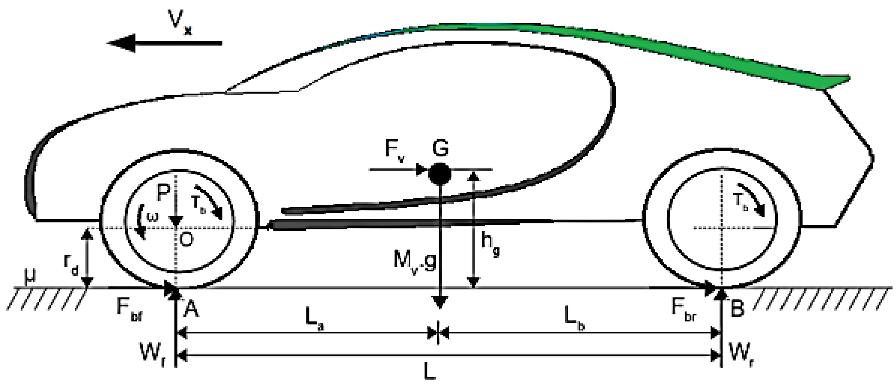

Figure 3.9 the brake operations are performed while vehicle is running on flat roads.

The stack will be moved from the rear wheels to the front wheels when the brake pedal is pushed on, which is able to influence the distribution of braking force between front and rear wheels [8, 19]. To estimate the impact of stack development on braking, brake quality z is characterized by the condition 3.10. Where, g is the gravitational acceleration (m/s ^2) and (αv) is the vehicle's deceleration

$$z = \frac{av}{g}$$
$$z = \frac{0.95}{9.81} = 0.096 \tag{14}$$

Thus, the maximum braking forces Fbf and Fbr which can be generated for the front and rear wheels, are given by Equations (3.13–3.15):

$$Fbf = \mu * Wf = \mu * \frac{Mv * g(L_b + z * hg)}{L}[N]$$

$$Fbf = \mu * Wf = 0.4 * \frac{1345*9.81(1.575 + 0.096 * 0.57)}{4.011} = 2144.43N \quad (3.15)$$

$$Fbr = \mu * \mathrm{Wr} = \mu * \frac{Mv * g(La - z * hg)}{L}$$

$$Fbr = \mu * \mathrm{Wr} = 0.4 * \frac{1345*9.81(1.572\mathrm{m} - 0.096*0.57)}{4.011} = 1996.5N \quad (3.16)$$

$$Fbf + Fbr = \mu * Mv * g$$

$$Fbf + Fbr = 0.4*1345*9.81 = 5{,}277.78\mathrm{N} \quad (3.17)$$

where Wf and Wr are the typical forces on the front and rear wheels, G is the overall load of the vehicle and μ speaks to the friction coefficient between the tire and the street surface. It is impossible to decide the braking strengths which can make the front and rear wheels lock for each friction coefficient. When the braking force is conveyed among the front and raise wheels secure braking is secured, which can be expressed as

$$Fbr = \frac{1}{2}\left[\frac{Mvg}{hg}\sqrt{Lb^2 + \frac{4hgL}{Mvg}Fbf} - \left(\frac{MvgLb}{hg} + 2Fbf\right)\right]$$

$$Fbr = \frac{1}{2}\left[\frac{1345*9.81}{0.57}\sqrt{1.575^2 + \frac{4*0.57*4.011}{1345*9.81}*5{,}277.78} - \left(\frac{1345*9.81*1.575}{0.57} + 2*5{,}277.78\right)\right] \quad (3.18)$$

$$= 0.5[23{,}148.45*(\sqrt{2.480625 + 352.03}) - (47013.9)]$$

$$= [217{,}919.5 - 23{,}506.95] = 194{,}412.55$$

The perfect braking force distribution characteristics were decided by calculations based on the determinations of a traveler vehicle (see Table 3.2). As shown in Equation (2.13) and Equation (2.16), braking forces and changes with the friction coefficient μ. Hence, in arrange to disperse braking force concurring to the ideal curve.

The changing friction coefficient directly. It can be found that the distribution ratio Rf and Rr of the front and rear wheels, does not depend on the friction coefficient [20].

$$Rf = \frac{Ff}{Ff + Fr} = \frac{Lb + Z * hg}{La + Lb} = \frac{1.575 + 0.096 * 0.57}{1.575 + 1.572} = 0.517 \quad (3.19)$$

$$Rr = 1 - Rf = 1 - 0.517 = 0.483 \quad (3.20)$$

The vehicle models available are of the following types: general vehicle model, vehicle model of four-wheels, vehicle model of two-wheels and vehicle model of the single wheel. The dynamic model with the four wheels in order to describe a suitable braking performance and also to simplify the underlying problem. The brake pedal is pressed against the brake plate, thus developing a frictional torque. This braking torque results in a braking force at the contact area between the tire and the ground. It is this braking force that tries to stop the vehicle. The traction or braking force is produced by the pneumatic tire and friction coefficient. Depending on the driver's command this is often satisfactory strategy given to EV protection device avoiding any overstated height of temperature and current peaks [21]. The braking forces act on front and rear wheels and can be expressed as the force (Fbf) available at the tire-ground contact which depends on the axle torque (Tb) and tire radio (rd). The wheel response force will produce a torque that starts rolling movement of the wheel, resulting in an angular speed ω. The equations of motion and longitudinal friction of the wheels are[20].

$$Me * av = Me * \frac{\delta Vx}{\delta t} \quad (3.21)$$

$$Fbf = \frac{Tb}{rd} \quad (3.22)$$

$$Fbf = \mu P \quad (3.23)$$

$$Fbf = \frac{Jw * \dot{\omega} + Tb}{rd} \quad (3.24)$$

Where Me is ¼ of the mass of the vehicle (kg), Vx is the vehicle speed (m/s), Fv is the longitudinal friction (N), Jw is the moment of inertia of the wheel (kg·m2), ω is the wheel angular speed (rd /s), rd is the wheel radius, Tb is the front brake torque (N-m), μ is the coefficient of longitudinal friction, and P is the normal force (N)

3.7. The Proposed Block Diagram of BLDC Motor Drive

The proposed system diagram of the speed control of the BLDC motor drive for the propulsion regenerative braking of battery electric vehicle is shown in Figure 3.9. The difference within the reference speed and actual rotor speed is controlled by employing a speed regulator. For this, a PSO based PID speed controller is proposed. Three phase reference current is generated from the speed controller output and hall sensor decoded signals. Usually, the motor needs this limiter thanks to the high starting current. Two phases of the stator current are taken because the stator current feedback because once the 2 current phases are known the third phase may be a negative summation of the 2 phases. The difference of phase current and also the corresponding reference current is controlled by using the PSO-PID controller. The motor armature current has harmonics and results in torque ripple. PWM consists of a comparator, output of the present controller converted to voltage, carrier signal including its switching frequency and also the logical circuit which is employed to come up with inverted riving signals. The inputs for PSO are illustrated in Table 3.6 which includes population size, maximum iteration, positions (C1, and C2), velocity (w), upper and lower bounds.

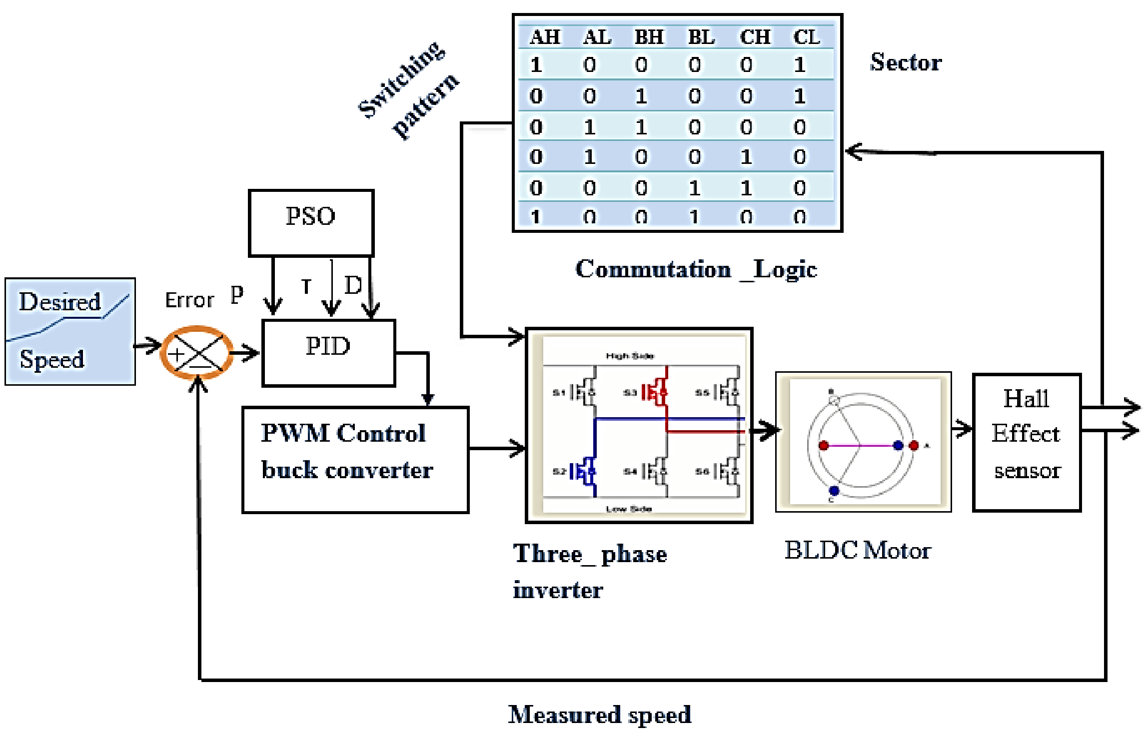

Figure 3.10 Speed control of BLD motor with PID_PSO control algorithm

Consider a motor with three coil windings in the stator and a single pole-pair in the rotor. This type of BLDC motor is driven by six-step commutation by a three-phase inverter where the correct phases are commutated every 60 degrees for continuous rotation of the motor. To learn more about six-step commutation and how it works the following figures are discussed as follow.

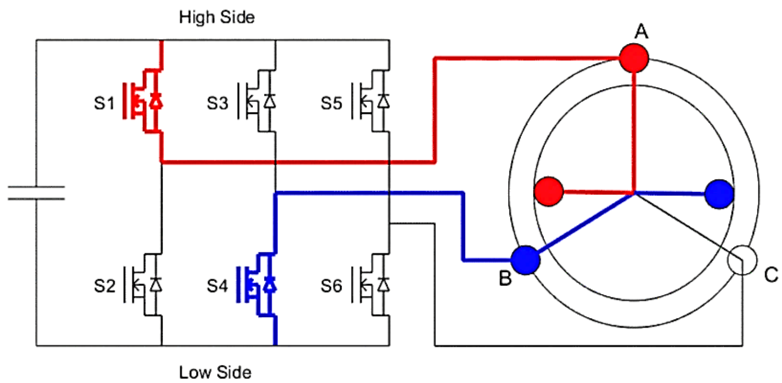

Figure 3.11 Working principle of 3phase inverter with BLDC

A DC voltage source provides a constant voltage to the three-phase inverter, which converts the DC power to three-phase currents to energize different coil pairs in turn.

As shown in the figure below when the applied voltage is constant (plot on the left) the engine turns at a steady speed (plot on the right) due to the proportionality voltage and speed.

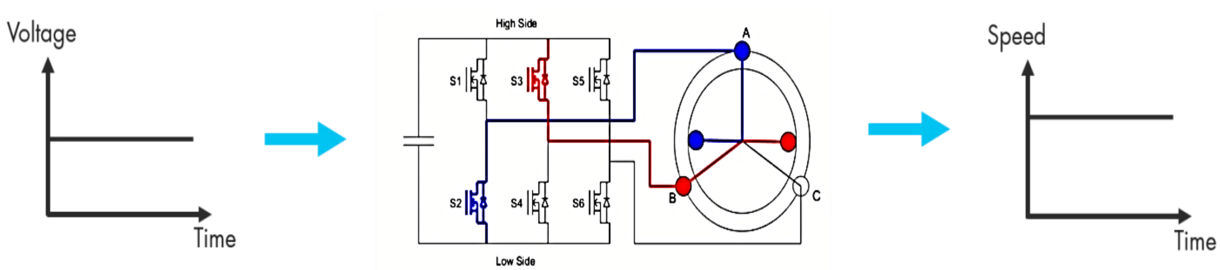

Figure 3.12 voltage -speed relationships for BLDC motor

However, if the motor to run at different speeds, a controller that will adjust the magnitude of the applied voltage. The following steps outline how to build this algorithm

3.7.1. Hall Sensors for Sector Detection

To control the rotor angular position and speed by using sensors like Hall Effect sensors. The Hall sensor does not give data on accurately where the rotor is inside a sector. Instead, it detects when the rotor transitions from one sector to another (figure 3.13), if the rotor is between 0 and 60 degrees, then it means the rotor is in the first sector and output1, similarly, there are more cases until complete the full rotation of the rotor. The angular position theta always between 0 and 360 degrees, which means that after every full rotation of the rotor again reset theta to 0 degrees. which is the only input that is needed to determine the commutation of the motor phases.

The correct phases are specified by a commutation logic circuit as discussed figure 3.14.

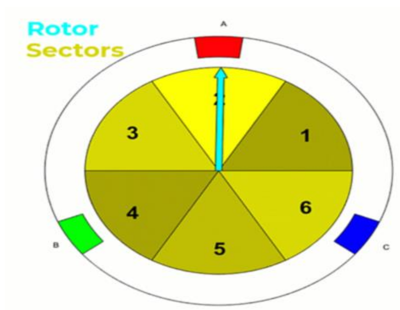

Figure 3.13 hall sensor

3.7.2. Commutating Phases with a Commutation Logic Circuit

Figure 3.14 shows how distinctive components of the motor control algorithm connected with each other. The commutation relational circuit computes the switching pattern for the three-phase inverter. Within the commutation logic table, the letters A, B, and C stand for the three phases of the motor. The high side of the three-phase inverter is labeled with H and the low side with L. In case the rotor is inside the primary segment, the commutation logic chooses the top switching pattern, which directs that the high side switch of phase A and the low side switch of phase C are turned on.

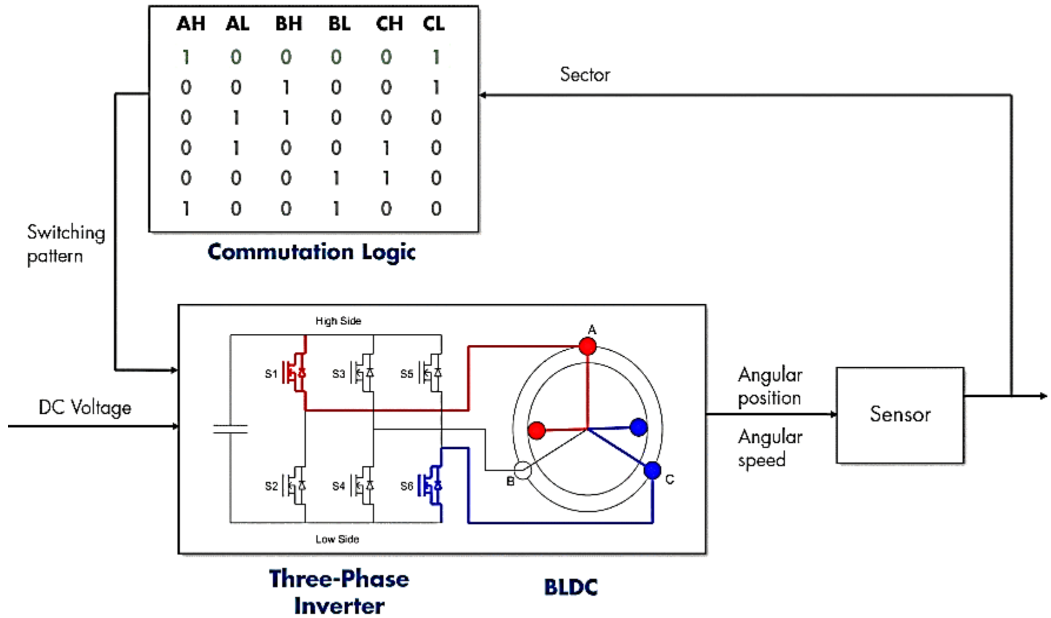

Figure 3.14 Interactions of commutating phases with a commutation logic circuit

As the rotor transitions to other sectors, the next switching pattern is selected accordingly and sent to the three-phase inverter. In summary, the sensor tells us when to commutate the rotor, and the commutation logic determines the correct phases to energize during each commutation. This way we're able to spin our motor. The next goal will be to enable the motor to spin at different speeds.

3.8. The BLDC Motor Mathematical Model

The BLDC motor Speed–torque performance is most vital for traction and other applications. As the other electric machine, the torque is generating by the interconnection of the magnetic flux and current. The field is produced in BLDC by the PM, and also the current depends on the source voltage, control, and also the back EMF, which is decided by the magnetic flux and speed of the machine. To get the required torque and speed at a given load, this must be controlled.

The performance analysis of BLDC machines have some Simplification [3][22]:

- Desaturated the motor
- Stator resistances of all the windings are equal, and self- and common inductance are constant. Power semiconductor gadgets within the inverter are ideal.

- Iron losses are negligible.

The BLDC motor phase equations is, taking into consideration the self and leakage inductances are expressed by:

$$
\begin{aligned}
V_a &= R_{aia} + \frac{d}{dt}\left[L_{aaia} + L_{baib} + L_{caic}\right] + E_a \\
V_b &= R_{bib} + \frac{d}{dt}\left[L_{abia} + L_{bbib} + L_{cbic}\right] + E_b \\
V_c &= R_{cic} + \frac{d}{dt}\left[L_{acia} + L_{bcib} + L_{ccic}\right] + E_c
\end{aligned}
\tag{3.25}
$$

where V_a , V_b and V_c are the stator voltage phases; i_a , i_b and i_c are the stator electric current; R_a , R_b and R_c are the winding resistances; L_{aa} , and L_{cc} are self-inductances of the stator; L_{ab} , L_{ba} , L_{bc} , L_{ca} , Lac and L_{cb} are the leakage inductances of each adjacent phase; and E_a , E_b and E_c are the back electromotive force of each phase. Considering that the phase windings are equal, hence Ra = $R_b = R_c = R$ (where R is the general resistance of the stator); L_{aa} = L_{bb} = L_{cc} = L (where L is the general self-inductance); Lab = Lac = L_{ba} = $L_{ca} = L_{cb}$ = M (where M is the general mutual inductance), whence one can obtain:

$$
\begin{aligned}
V_a &= Ri_a + \frac{d}{dt}\left[Lia + Mib + Mic\right] + E_a \\
V_b &= Ri_b + \frac{d}{dt}\left[Mia + Lib + Mic\right] + E_b \\
V_c &= Ri_c + \frac{d}{dt}\left[Mia + Mib + Lic\right] + E_c
\end{aligned}
\tag{3.26}
$$

For a balanced system, then the currents $ia + ib + ic$ = 0; deriving the previous equation returns, $\frac{di_a}{dt} + \frac{di_b}{dt} + \frac{di_c}{dt} = 0$ and $-\frac{dia}{dt} = \frac{dib}{dt} + \frac{dic}{dt}, -\frac{dib}{dt} = \frac{dia}{dt} + \frac{dic}{dt}, -\frac{dic}{dt} = \frac{dib}{dt} + \frac{dia}{dt}$; replacing the derivatives in (3.26) respectively, yields:

$$
\begin{aligned}
V_a &= Ri_a + \frac{di_a}{dt}\left[L - M\right] + E_a \\
V_b &= Ri_b + \frac{di_b}{dt}\left[L - M\right] + E_b \\
V_c &= Ri_c + \frac{di_c}{dt}\left[L - M\right] + E_c
\end{aligned}
\tag{3.27}
$$

From (3.27) it is possible to infer the comparable circuit of the BLDC motor, as appeared in Figure (3.14) [1].

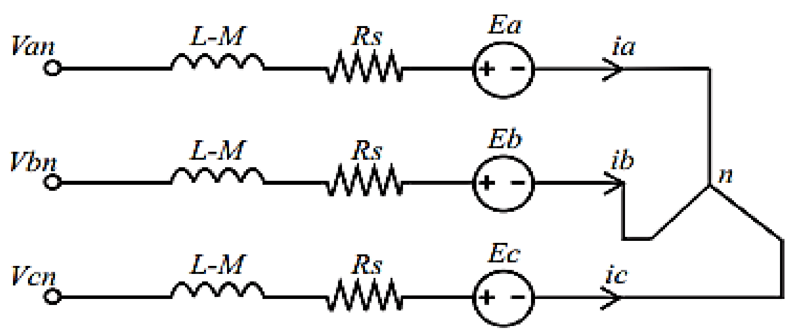

Figure 3.15 BLDC motor equivalent circuit.

The simplified stator equations can be obtained by doing $Ls = L - M$, thus: The overall electromagnetic torque created by the stage streams is express by

$$
\begin{aligned}
V_a &= Ri_a + \frac{d}{dt}L_s i_a + E_a \\
V_b &= Ri_b + \frac{d}{dt}L_s i_b + E_b \\
V_c &= Ri_c + \frac{d}{dt}L_s i_c + E_c
\end{aligned}
\tag{3.28}
$$

$$
Te = \frac{E_a i_a + E_b i_b + E_c i_c}{\omega_m} \tag{3.29}
$$

The EMF induced in each phase is given as:

$$
\begin{aligned}
E_a &= fa(\theta r)\lambda p\omega m \\
E_b &= fb(\theta r)\lambda p\omega m \\
E_c &= fc(\theta r)\lambda p\omega m
\end{aligned}
\tag{3.30}
$$

where λp is the flux constant and the functions $fa(\theta r)$, $fb(\theta r)$ and $fc(\theta r)$ represent the profile of Ea, Eb and Ec with magnitudes closed to ±1, as expressed in (3.30). By replacing in (3.29), the electromagnetic torque, in $N.m$, is written as:

$$Te = \lambda p\left[fa(\theta r)ia + fb(\theta r)ib + fc(\theta r)ic \right] \tag{3.31}$$

The dynamic equation for a system with inertia J, friction coefficient B, and load torque Tl is given by:

$$J\frac{d\omega r}{dt} + B\omega r = \left(Te - Tl\right) \tag{3.32}$$

Where at the speed of rotor and their position are related to each other by:

$$\frac{d\theta r}{dt} = \frac{P}{2}\omega r \tag{3.33}$$

Where P indicate that the number of poles, ωr is the rotor speed in rad/s, and θr is the rotor position. From the previous equations, the set of differential equations that represents the modeling of a BLDC motor is expressed by:

$$\begin{aligned} \frac{di_a}{dt} &= -\frac{Ri_a}{L-M} + \frac{V_a}{L-M} - \frac{E_a}{L-M} \\ \frac{di_b}{dt} &= -\frac{Ri_b}{L-M} + \frac{V_b}{L-M} - \frac{E_b}{L-M} \\ \frac{di_c}{dt} &= -\frac{Ri_c}{L-M} + \frac{V_c}{L-M} - \frac{E_c}{L-M} \end{aligned} \tag{3.34}$$

$$\begin{aligned} \frac{d\omega_r}{dt} &= -\frac{B\omega_r}{J} - \frac{T_l}{J} + T_e \\ \frac{d\omega_r}{dt} &= \frac{P}{2}\theta_r \end{aligned} \tag{3.35}$$

Substitute Equation (3.30) in (3.34) and rewrite the equation

$$\begin{aligned}\frac{di_a}{dt} &= -\frac{Ri_a}{L-M} + \frac{V_a}{L-M} - \frac{f_a(\theta_r)\lambda_p\omega_m}{L-M}\\ \frac{di_b}{dt} &= -\frac{Ri_b}{L-M} + \frac{V_b}{L-M} - \frac{f_b(\theta_r)\lambda_p\omega_m}{L-M}\\ \frac{di_c}{dt} &= -\frac{Ri_c}{L-M} + \frac{V_c}{L-M} - \frac{f_c(\theta_r)\lambda_p\omega_m}{L-M}\end{aligned} \tag{3.36}$$

$$\frac{d\omega_r}{dt} = -\frac{B\omega_r}{J} - \frac{T_l}{J} + \frac{\lambda_p\left[f_a(\theta_r)i_a + f_b(\theta_r)i_b + f_c(\theta_r)i_c\right]}{J} \tag{3.37}$$

$$\frac{d\theta_r}{dt} = \frac{P}{2}\omega_r \tag{3.38}$$

Equations (3.36), (3.37) and (3.38) can be represented in the form of a matrix as:

$$\dot{x}^T = \begin{bmatrix} \dot{i}a(t) & \dot{i}b(t) & \dot{i}c(t) & \dot{\omega}r(t) & \dot{\theta}r(t) \end{bmatrix}, \text{ and}$$

$$\frac{d}{dt}\begin{bmatrix} i_a \\ i_b \\ i_c \\ \omega_r \\ \theta_r \end{bmatrix} = \begin{bmatrix} \frac{-R}{L-M} & 0 & 0 & \frac{\lambda_p f_a(\theta_r) i_a}{L-M} & 0 \\ 0 & \frac{-R}{L-M} & 0 & \frac{\lambda_p f_b(\theta_r) i_b}{L-M} & 0 \\ 0 & 0 & \frac{-R}{L-M} & \frac{\lambda_p f_c(\theta_r) i_c}{L-M} & 0 \\ \frac{\lambda_p f_a(\theta r) i_a}{J} & \frac{\lambda_p f_b(\theta r) i_b}{J} & \frac{\lambda_p f_c(\theta r) i_c}{J} & \frac{-B}{J} & 0 \\ 0 & 0 & 0 & 0 & \frac{P}{2} \end{bmatrix} \begin{bmatrix} i_a(t) \\ i_b(t) \\ i_c(t) \\ \omega_r(t) \\ \theta_r(t) \end{bmatrix} + \begin{bmatrix} \frac{1}{L-M} & 0 & 0 & 0 \\ 0 & \frac{1}{L-M} & 0 & 0 \\ 0 & 0 & \frac{1}{L-M} & 0 \\ 0 & 0 & 0 & \frac{-1}{J} \\ 0 & 0 & 0 & 0 \end{bmatrix} \begin{bmatrix} V_a(t) \\ V_b(t) \\ V_c(t) \\ T_L \end{bmatrix} \tag{3.39}$$

The state space form is given below

$$\dot{x} = AX + Bu \tag{3.40}$$

where

$$A=\begin{bmatrix} \frac{-R}{L-M} & 0 & 0 & \frac{\lambda_p f_a(\theta_r) i_a}{L-M} & 0 \\ 0 & \frac{-R}{L-M} & 0 & \frac{\lambda_p f_b(\theta_r) i_b}{L-M} & 0 \\ 0 & 0 & \frac{-R}{L-M} & \frac{\lambda_p f_c(\theta_r) i_c}{L-M} & 0 \\ \frac{\lambda p f a(\theta r) i_a}{J} & \frac{\lambda p f b(\theta r) i_b}{J} & \frac{\lambda p f c(\theta r) i_c}{J} & \frac{-B}{J} & 0 \\ 0 & 0 & 0 & 0 & \frac{P}{2} \end{bmatrix}, B=\begin{bmatrix} \frac{1}{L-M} & 0 & 0 & 0 \\ 0 & \frac{1}{L-M} & 0 & 0 \\ 0 & 0 & \frac{1}{L-M} & 0 \\ 0 & 0 & 0 & \frac{-1}{J} \\ 0 & 0 & 0 & 0 \end{bmatrix}, x=\begin{bmatrix} i_a(t) \\ i_b(t) \\ i_c(t) \\ \omega_r(t) \\ \theta_r(t) \end{bmatrix}, u=\begin{bmatrix} V_a(t) \\ V_b(t) \\ V_c(t) \\ T_L \end{bmatrix}$$

Where V_a , V_b and V_c are the phase voltages in volts, stator winding resistance is denoted by R in ohms. i_a , i_b and i_c indicate the phase streams of the motor in amperes. L and M in Henry indicate the self-inductance of the motor winding and the mutual inductances between stator windings, respectively e_a , e_b and e_c represent the back electromagnetic constrain of each stage in volts. The number of posts within the rotor is represented by P, and θ_r is the rotor position of the rotor in radians. J, B, ω_r , and TL represent the moment of inertia, frictional coefficient, angular velocity, and load torque of the motor, respectively. The equation of torque is given as in (3.41)

$$T_e = B\omega_r + J\frac{d\omega_r}{dt} + T_L \tag{3.41}$$

3.8.1. Modeling of Ideal Back-EMF

The profiles of the ideal three phases EMF are shifted from one another by 120◦.[23] .The BLDC motor back-EMF can be described by from the Equations (3.42).

Where λp is the flux constant, θr electrical rotor angle , ωm is the rotor speed in rad/s and the functions $fa(\theta r)$, $fb(\theta r)$ and $fc(\theta r)$ represent the profile of E_a , E_b and E_c with magnitudes closed to ±1. Equations (3.42), (3.43), and (3.44) show the mathematical functions of the rotor angle in a three-phase system.

$$fa(\theta r) = \begin{cases} 1, & 0 < \theta r \le \frac{\pi}{3} \\ \left(\frac{\pi}{3} - \theta r\right) * \frac{6}{\pi}, & \frac{\pi}{3} < \theta r \le \frac{2\pi}{3} \\ -1, & \frac{2\pi}{3} < \theta r \le \pi \\ -1, & \pi < \theta r \le \frac{4\pi}{3} \\ \left(\theta r - \frac{3\pi}{2}\right), & \frac{4\pi}{3} < \theta r \le \frac{5\pi}{3} \\ 1, & \frac{5\pi}{3} < \theta r \le 2\pi \end{cases} \tag{3.42}$$

Similarly

$$fb(\theta r) = fa\left(\theta r + 2\frac{\pi}{3}\right) \tag{3.43}$$

$$fc(\theta r) = fa\left(\theta r - 2\frac{\pi}{3}\right) \tag{3.44}$$

The induced emf does not have sharp corners, but it has rounded edges. The emf produced are the result of the flux linkage derivatives which is a continuous function.

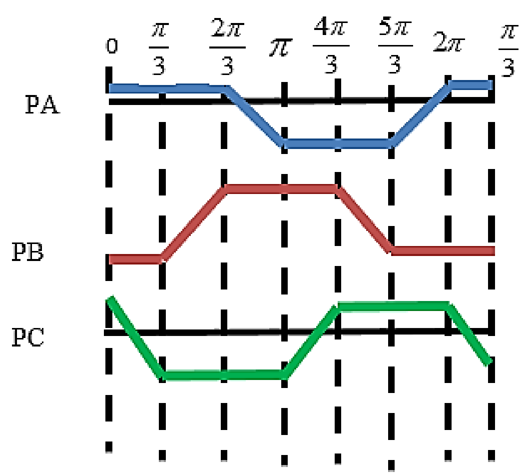

Figure 3.16 Back EMF model for BLDC

Modeling Hall Effect Signals and Inverter Switches Status of the BLDC Motor Mostly, three Hall Effect sensors are present in BLDCM which are at 120 degrees apart [6][24]. Whenever the rotor passes through the sensor, it gives logic state HIGH. Else it remains at logic state LOW. Each sensor is active for 180 degrees in each cycle.

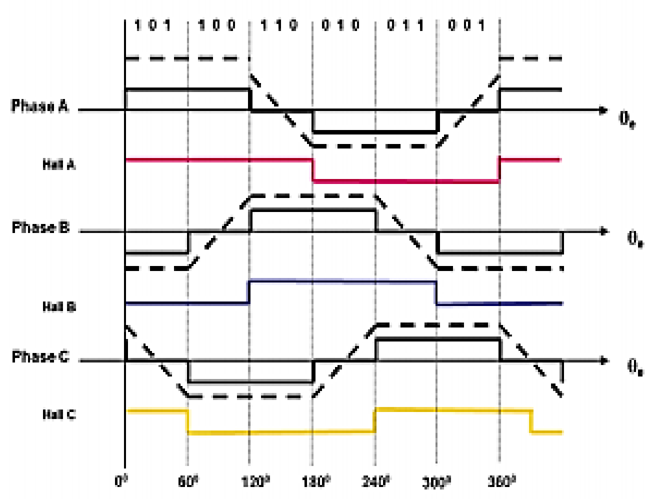

Figure 3.17 Waveforms of phase and hall sensor signals

For controlling BLDC motor, the H-Bridge inverter is usually used [8][25]. To energize windings to rotate the rotor, appropriate switches have to be turned ON. During 0-60 degrees of Figure.15, phase A and phase B should be turned ON and phase C is at floating state. So, to show ON A and B phase coils, S1 and S2 of figure3.17 should be turned ON. No two switches of same leg of inverter should activate simultaneously.

Table 3.5 The inverter switching sequence[25]

Hall A	Hall B	Hall C	A	B	C	S1	S2	S3	S4	S5	S6
1	0	1	+1	-1	0	1	0	0	0	0	1
1	0	0	+	0	-1	1	1	0	0	0	0
1	1	0	0	+1	-1	0	1	1	0	0	0
0	1	0	-1	+1	0	0	0	1	0	0	0
0	1	1	-1	0	+1	0	0	0	1	1	0
0	0	1	0	-1	+1	0	0	0	1	1	1

Top switch of 1 leg and bottom switch of another leg should activate simultaneously. Under motoring mode, all the six switches of inverter are in use. Controller takes hall sensor states as reference and generates in Table (3.5) shows BLDCM inverter switching sequence for motoring mode.

Gating pulses to turn ON appropriate switches inverter of BLDCM for motoring mode.in the low power range and in applications requiring variable speed control, adopting BLDC motor can cause efficiency improvements of up to 10% to fifteen compared with AC induction motors, and permit the likelihood of 90% operating efficiency[25]. At the identical time, BLDC motors are more energy productive than induction motor, because of the motors eliminate the excitation circuit losses and doesn't suffer from friction because of the brushes.

3.9. Controller Design

3.9.1. PID Controller

The PID (Proportional integral derivative) controller is that the common and useful algorithm on top of engineering system in most case, feedback Closed loop system are controlled by PID control algorithm. the main reason why feedback loops is incredibly important for the systems to be ready to attain a collection –point regardless of disturbance or any variation in characteristics of any form. The PID controller is usually designed to correct errors (e) between measured process values and particular desired set-point in an exceedingly system. An easy construct work of PID controller is as follow. The proportional (P), Integral (I) and derivative (D) controls, as shown to the block diagram in Figure 3.18 The system, S is to be controlled using the controller C; where controller, C efficiency of depends on P, I, D parameters]

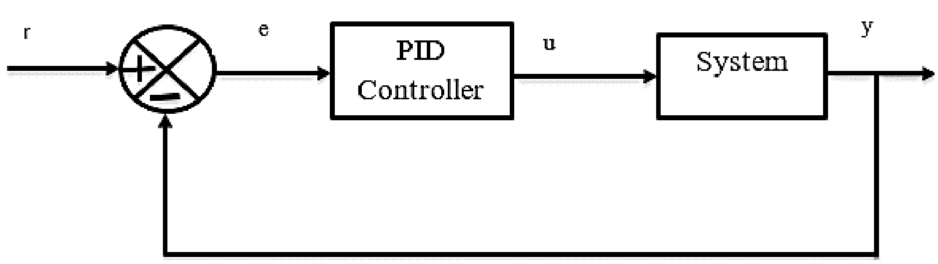

Figure 3.18 Feedback control loop, block diagram

The controller provides the excitation need by the system and it's designed to regulate the general behavior of the system. The PID controller has several categories of the structure arrangements. The foremost common of those are the series and parallel structure and, in some case, there are the hybrid sort of the series and parallel structures. Consider the figure 3.18 e is that the sample error and it's the difference between the specified input value R and the particular output value Y, .In closed-loop system e will sent to the controller and also the controller will perform the integral and derivative computation on the error signal. Thereafter, the output of the controller (u) is now adequate the sum of the product of proportional gain, KP and also the magnitude of the error, the merchandise of integral gain, KI and therefore the integral of the error and the product of derivative l gain, KD and therefore the derivative of the error. That is

$$U = KPe + KI\int edt + KD\frac{de}{dt} \tag{3.45}$$

Where K_P = proportional gain, K_I =integral gain and K_D = derivative gain

The signal value, u sent the signal continuously to the plant corresponding to the new output Y being the process continues. The output Y, sent to back and subsequently new error signal, e is found and the same process repeats itself on and on.

3.9.2. Application of PSO for Controller Parameters Tuning

PSO is one in every of the optimizations yet as a form of evolutionary computation technique. This optimization has been used to be robust in solving problems which have different properties like nonlinearity and non-differentiability, multiple optima, and high dimensionality through adaptation, which comes from the social-psychological theory [26]. Its technique comes from research on swarm like fish schooling and bird flocking. Per the research results for a flock of birds, birds find food by flocking (not by each individual) and observation leads the belief that each information is shared inside flocking. Moreover, in line with observation of behavior of human groups, behavior of every individual (agent) is additionally supported behavior patterns authorized by the groups. The customs and other behavior patterns consistent with the experiences by each individual and assumption may be a basic concept of PSO.

Within the PSO algorithm, rather than using evolutionary operators like mutation and crossover, to govern algorithms, for a d-variable optimization problem, a flock of particles are put into the d-dimensional search space with randomly chosen velocities and positions knowing their best values thus far (Pbest) and therefore the position within the d-dimensional space. The velocity of each particle, adjusted according to its own flying experience and the other particle's flying experience. For example, the i[th] particle is represented $xi=(xi,1,xi,2,\ldots,xi,d)$ in the d-dimensional space. The best previous position of the i[th] particle is recorded and represented as: $Pbesti = Pbesti,1, Pbesti,2,\ldots, Pbesti,d$ The index of best particle among all of the particles in the group $gbest_d$ is the velocity for particle i is represented as $V_i = V_{i,1}, V_{i,2} \ldots V_{i,d}$ The modified velocity and position of each particle can be calculated using the current velocity and the distance from $gbest_{i,d}$ to $Pbest_d$ as shown in the following formulas [27].

$$V_{i,m}^{(i+1)} = w.v_{i,m}^{(i+1)} + c_1 * Rand() * (pbest_{i,m} - x_{i,m}^{(t)}) + c_2 * Rand() * (gbest_m - x_{i,m}^{(t)}) \quad (3.45)$$

$$x_{i,m}^{(i+1)} = x_{i,m}^{(t)} + v_{i,m}^{(t+1)} \quad , \quad i = 1,2,\ldots.n \quad m=1,2,\ldots.n \quad (3.46)$$

where n= number of in the group,d=dimension,t=pointer of iterations (generation) and $v_{i,m}^{(t)}$ =Velocity of particle ith iteration t $v_d^{(\min)} \le v_{i,d}^{(t)} \le v_d^{(\max)}$ rand () =random number between 0 and 1,W=inertia Weight factor ,C1, C2=acceleration constant $x_{i,d}^{(t)}$ = current position of particle i at iterations, $Pbest_i$ =best previous position of the i[th] particle and $gbest$ =best particle among all the particle in the population

3.9.3. PSO-PID Controller

Integral Absolute Error (IAE) is the most common criteria of performance for a PID controller, the integrated of time weight square error (ITSE) and integrated of squared error (ISE) that may be evaluated analytically within the frequency domain. This integral performance criteria within the frequency domain have advantage and their own and downsides [28]. The demerits of the IAE and ISE criteria is that its minimization may end up in an exceedingly response with approximately little overshoot but a protracted settling time because the ISE performance criteria's weights all errors equally independent of your time. In spite of the fact that the ITSE execution measure can overcome the drawback of the ISE criterion, the derivation forms of the analytical equation are complex and time-consuming [22]. The IAE, ISE, and ITSE execution basis equations are explained below:

$$IAE = \int_0^\infty |r(t) - y(t)| dt = \int_0^\infty |e(t)| dt \tag{3.47}$$

$$ISE = \int_0^\infty e^2(t) dt \tag{3.48}$$

$$ISTE = \int_0^\infty t e^2(t) dt \tag{3.49}$$

In this paper a time domain criterion is used for evaluating the PID controller [29].

A set of great control parameters P, I and D can yield a great step response that will result in performance criteria minimization within the time domain. The time domain incorporates the overshoot, rise time, settling time, and steady-state error are primary criteria. Subsequently, the performance criteria is characterized as follows [24]:

$$\min_{Kstablizing} W_K = (1 - e^{-\beta}) * (M_p + E_{ss}) + e^{-\beta} * (t_s - t_r) \tag{3.50}$$

where K is [P, I, D], and β is the weighting factor.

The performance criteria W (K) can fulfill the designing prerequisite using the weighting factor β value. β can set to be bigger than 0.7 to decrease the overshoot and steady states error, also can set smaller than 0.7 to decrease the rise time and settling time [20]. The choice of β depends on the designer's requirement and the characteristics of the plant under control. In BLDC motor speed control framework, the lower β would lead to more ideal response. In this thesis, due to trials, β is set to 0.5 to ideal the step response of speed control system. The fitness function is complementary of the performance criterion, within the other words:

$$f = \frac{1}{W(K)} \tag{3.51}$$

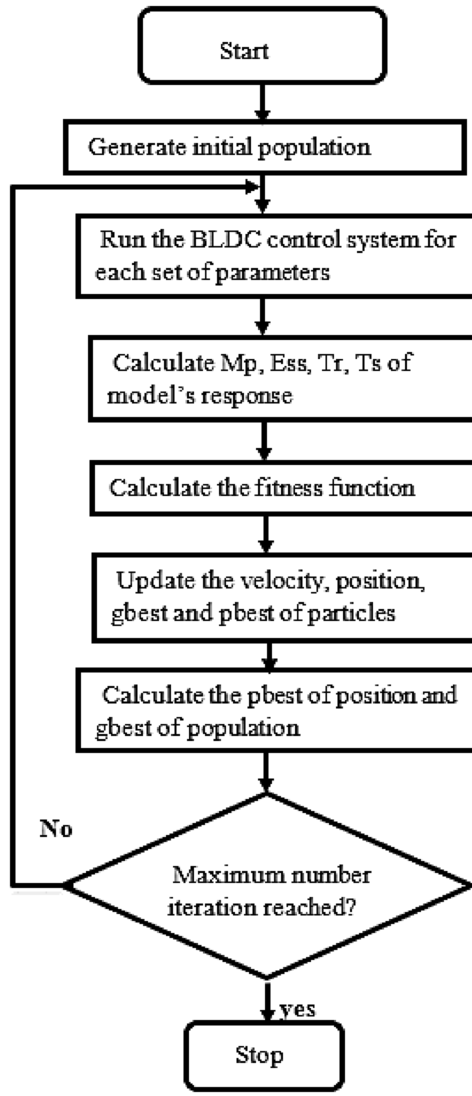

Figure 3.19 Flow chart of the PSO-PID Control system

Control parameters for the PSO algorithm to tune the PID controller are presented in Table 3.6

Table 3.6 PSO control parameters and the corresponding values.

Parameter	Value
Population size	20
Maximum iteration	30
C1	1
C2	2
w	1
Lower Bound	[0.001 0.001 0.001]
Upper Bound	[300 500 3.5]

With the given control parameter values in Table 3.6 and the flow chart in Figure 3.20, tuning PID controller parameters has been done. Accordingly, Figure 3.20 shows the convergence curve.

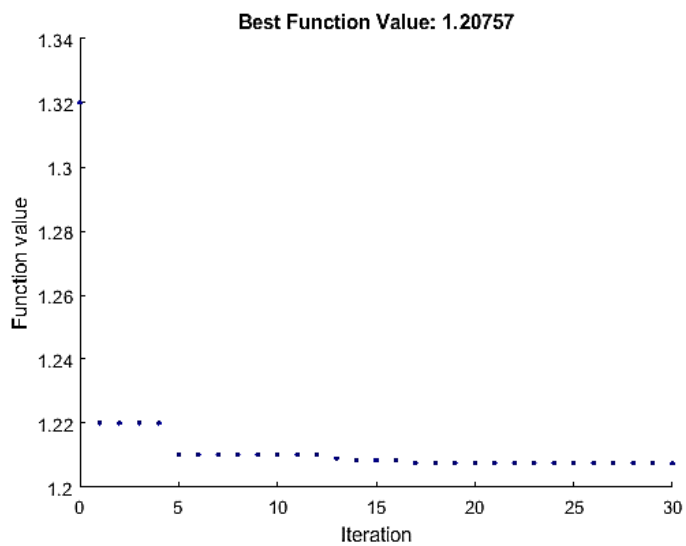

Figure 3.20 Optimization result of PSO-PID tuning

Figure 3.20 shows the tuning process of PID parameter using PSO algorithm for approximating the desired and measured speed of the BLDC motor to gate accurate result of measure speed compared to the above a tuned result. From the tuning process, the PID performance function KP KI KD ([1 1 1]) and the objective function value or Eval equal to 247. 3775.After completing the optimization process of PID controller by PSO, at the maximum iteration of 30

The best particle after optimization ended a number of iterations exceed optimized value of KP Ki KD ([1 1 1]) become KP KI KD ([200.0000 400.0000   2.9572]).and the objective function after optimization or Eval become 1.2076

3.9.4. Relay Based BLDC Motor Drive Hysteresis Current Controller

Hysteresis current control may be a strategy of creating the specified activating pulses by comparing the error signal with that of the hysteresis band and it is used for controlling the voltage source inverter so that the yield current is generated from the filter will take after the reference current waveform is shown in Figure 3.21.

This strategy controls the switches of the voltage source inverter no asynchronously to ramp the current through the inductor up and down, so that it takes after the reference current. Hysteresis current control is the simpler control to execute within the real time. Figure 3.21 outlines the ramping of the current between the two limits where the upper hysteresis limit is the addition of the reference current and the most extreme error or the difference between the upper limit and the reference current and for the lower hysteresis limit, it is the subtraction of the reference current and the minimum error.

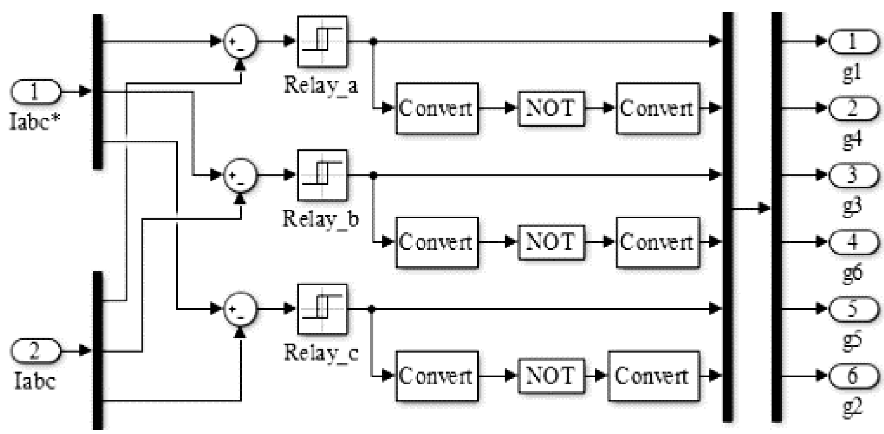

Figure 3.21 Relay based BLDC motor drive hysteresis current controller

Assuming the value for the least and greatest error should to be the same. As a result, the hysteresis band width is equal to two times of error. It works based on the comparison between the stator current and the reference current. The error signal is given to a two-level relay comparator moreover called hysteresis band comparator. Each phase requires one relay comparator. The output of the relay comparator gets to be one or zero based on the bandwidth of the relay. This control is hysteresis control. Figure 3.21 shows the usage of switching signal formation in Simulink. The output of relay comparator is associated to the logical NOT in each phase for switching the semiconductor within the same legs. When the upper switch is ON the lower switch should be OFF and vice versa under the same leg of the inverter.

CHAPTER FOUR

4. RESULTS AND DISCUSSION

The simulation results explained in this chapter is performed for the same values of the system parameters under study. The Simulation is done for confirming the viability of PSO tuned PID controller, the simulation results in Figure 4.1 that compared with the classical PID controller, this controller tune by PSO and found a better improvement in the performance characteristic. The system is simulated at the load torque of 250Nm and the speed response of BLDC Motor at 4800 rpm with PID and PSO tuned PID controller.

4.1. The Proposed BLDC Motor with Regenerative Braking Control Result

4.1.1. The Proposed Control System Results of BLDC Motor

In this work, the PSO-PID and hysteresis current controller with PWM based BLDC motor drive are proposed. The results are explained in detail in the following sections.

4.1.1.1. PSO Based PID Speed Controller Result of BLDCM with Regenerative Braking

Figure 4.1 shows the desired or reference motor speed to test the performance of the actual speed with controller and without controller. It follows different path with increasing and decreasing speed value for motoring and regenerative braking. It also shows that the performance of PID controller on the measured or actual speed with reference to the desired speed without PSO tuning.as seen from the result at the time of 0.5sec 0.8sec there is an overshoot of the measured speed and also in different path the measured speed does not exactly following the reference or desired speed path. This is because of the auto tuning of PID controller that creates different errors. And PID controller without controller have poor performance than PSO PID controller, settling time 0.08 and a rise time of 0.283sec. Due to this case for the proposed system of the BMW i3 vehicle speed is greater that the proposed seed at 0.6sec.at this time the speed is greater than 4800 rev/min.

In Figure 4.1, It is the result of desired and measured or actual speed result of BLDC motor after optimizing the parameters of PID controller with particles swarm optimization (PSO).

From Figure 4.1, it is shown that the actual or measured speed of BLDC motor is exactly follows the desired speed trajectory with Kp Ki Kd ([200.0000 400.0000   2.9572]) parameters of PID controller as tuned have 0% overshoot,0sec settling time and rise time 0.28sec. With this performance characteristics, Figure 4.1 result has more accurate for driving BLDC motor since this result have no more overshoot and have no time delay to follow the desired speed trajectory.

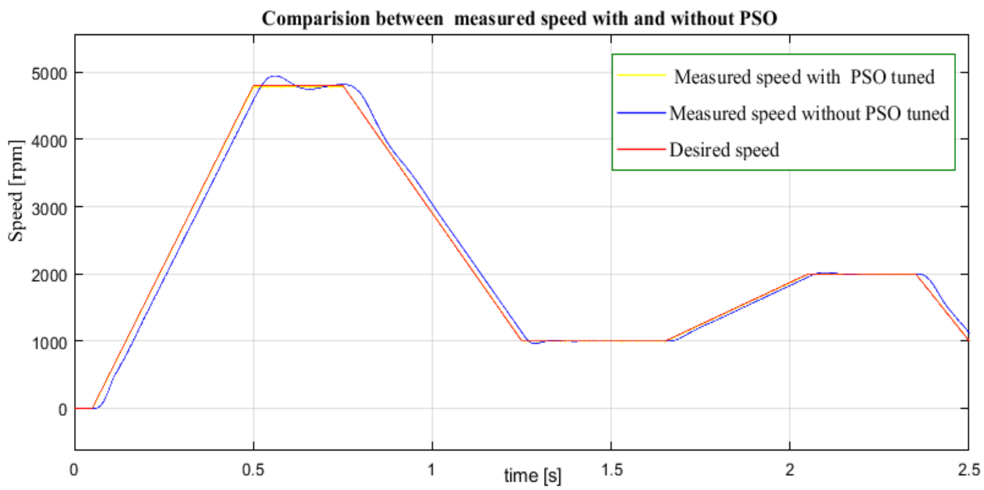

Figure 4. 1 Measured speed response with and without PSO

Furthermore, when the proposed system controlled with PID controller with and without PSO. The blue line shows the measured speed without PSO with having an overshoot at each phase. And the light red it the measured speed with PSO tuning of PID controller. It directly lines up with the reference speed for BLDC motor.

4.1.1.2. Current response in hall sensor

Figure 4.2 shows that the output result of current from the combined signal of hall sensor and speed controller. As seen from here the current output have harmonics with different signal amplitude at different time. It is known that the stator current frequency is directly proportional to the motor speed. From Figure 4.1, it is observed that the motor speed is increased from 0.2sec to 0.75sec. Hence, more harmonic exists from 0.2sec to 0. 75sec. After 0.75sec the three current signals have similar amplitude and similar frequencies. These three phase currents are given to the hysteresis controller as an input. Figure 4.2 is the zoomed result of current result which run from 0sec to 1.5sec from the total simulation time of 2.5sec.

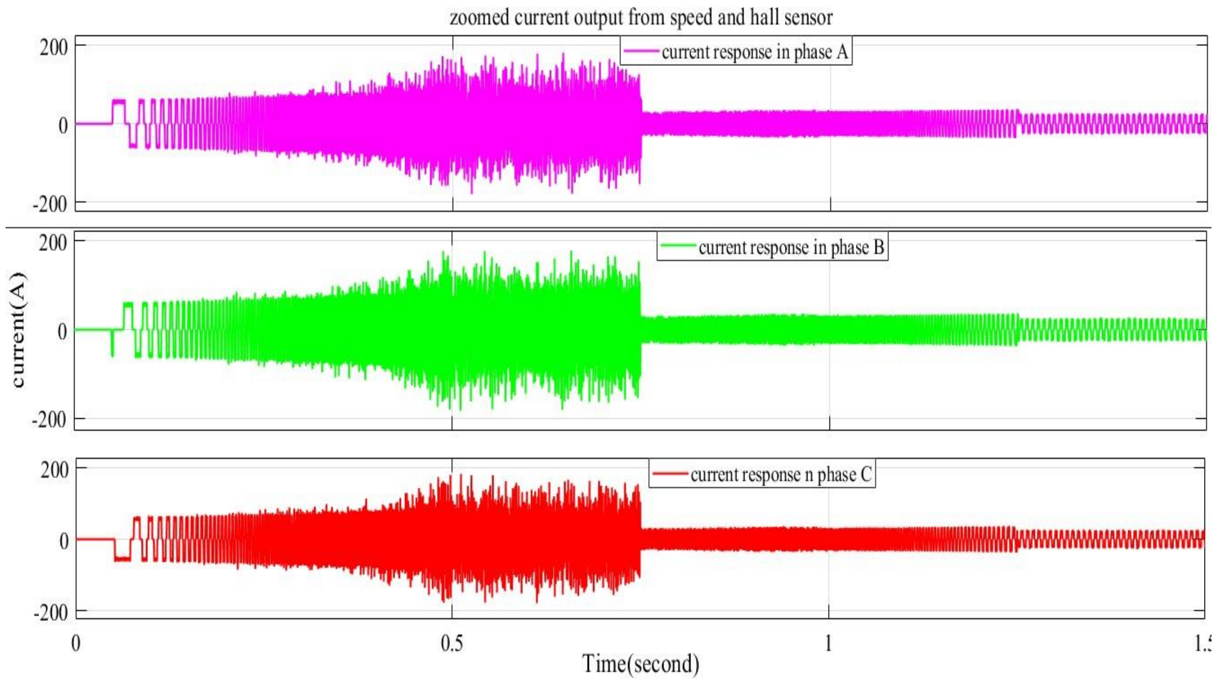

Figure 4. 2 Current response from speed and hall sensor signal

4.1.2. BLDC Drive Output Result

4.1.2.1. BLDCM Stator Current Result

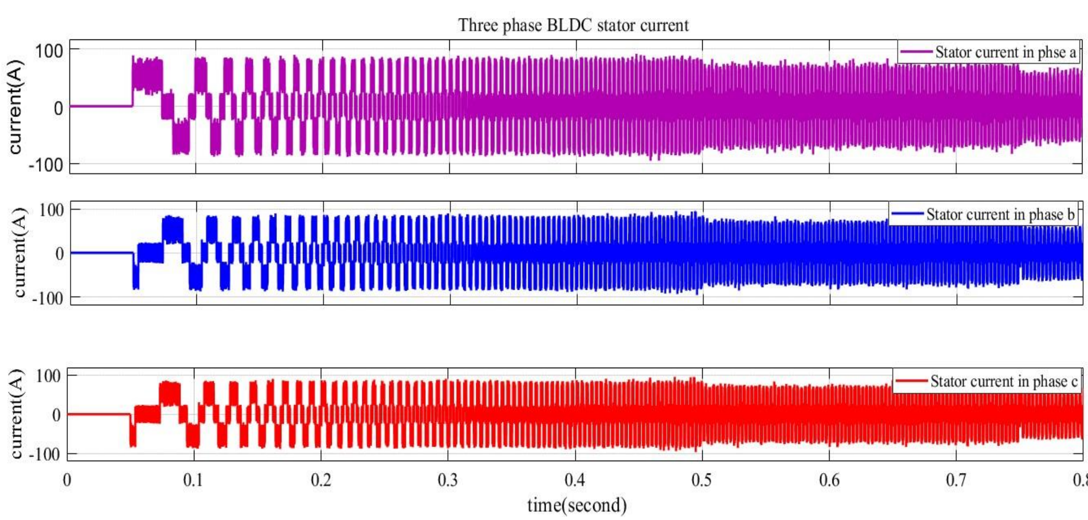

Figure 4. 3.Three phase stator current

Figure 4.3 is the stator current result, this current mostly contains harmonics. This harmonic is reduced to low value. This current of BLDC motor mostly generated under

PWM with low harmonic percentage. The frequency of stator current and stator voltage is directly proportional. That means if the frequency of stator current is increasing then the rotor speed or motor speed become increase. Since the motor speed stop varying and become constant at 0.5sec as shown in Figure 4.1, the magnitude of the three-phase stator current is changed at 0.5sec and the harmonics are decreased due to constant motor speed as illustrated in Figure 4.3.

4.1.2.2. BLDCM Three Phase Back-EMF Result

The three phase BLDC motor back-EM waveform result is generated shown in Figure 4.4 below. From this result, when the speed is increasing the induced back-EMF is also increasing. As an example, from the simulation time of 0 to 0.5sec the speed is increasing correspondingly the induced back-EMF is also increasing. And also, from 0.5sec to 0.75sec the speed is 4800rpm as represented in Figure 4.1 and the back-EMF is above 10V which is both speed and back emf are constant in the time interval between 0.5sec to 0.75sec. This result shows that the speed and induced back EMF voltage are directly proportional to each other.

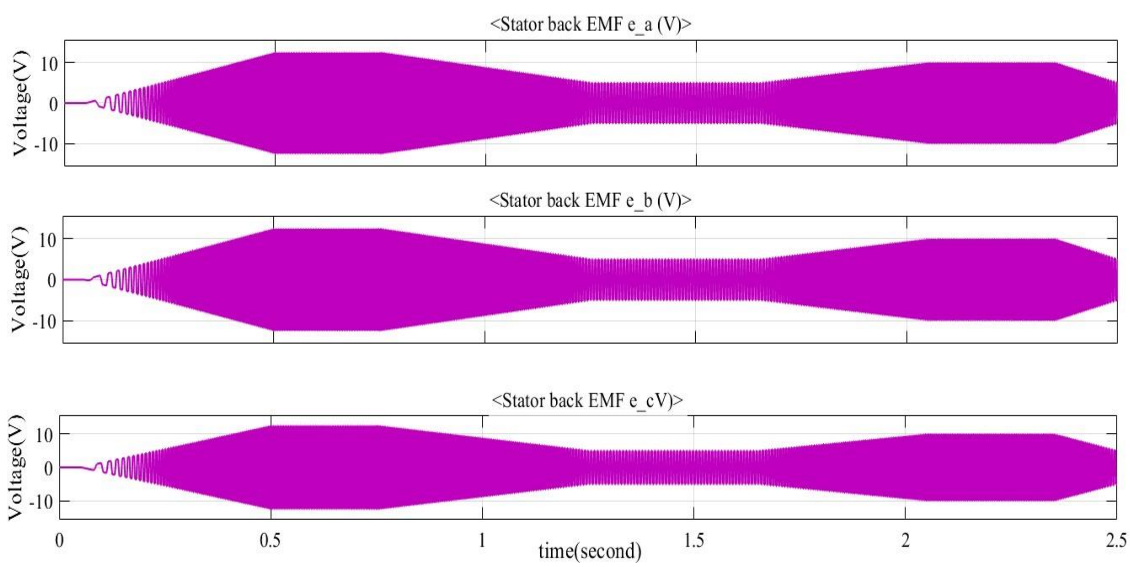

Figure 4. 4 Three phase stator back emf

4.1.2.3. BLDCM Electromagnetic Torque Result

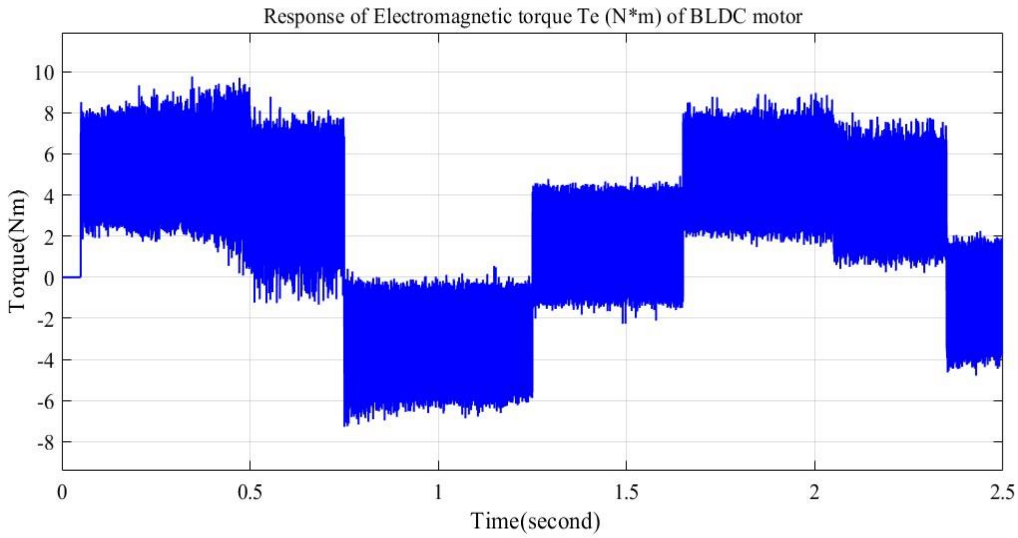

Figure 4. 5 Electromagnetic torque for BLDC motor

The electromagnetic torque and stator current of BLDC motor are directly proportional to each other. As a result, the stator current harmonics of the BLDC motor leads to torque ripple. Figure 4.5 explains the result of electromagnetic torque in MATLAB/Simulink drive system. The result shows it is proportional to the stator current. This figure shows the electromagnetic torque have the negative and positive pulses.at this different region BLDC motor have motoring and regenerative operation. When the speed is positive and torque is positive the BLDC motor runs in motoring mode but when torque is negative with positive speed it is regenerative.

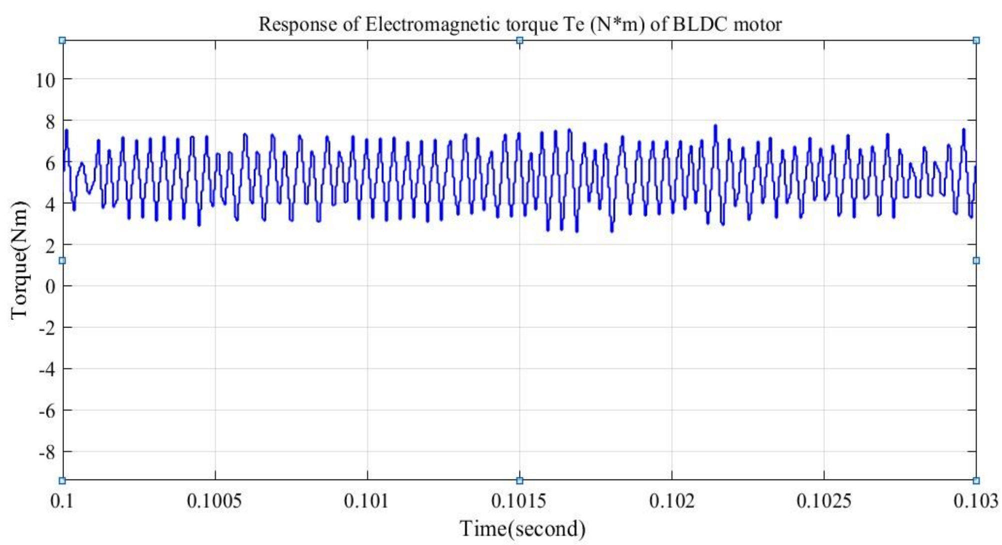

Figure 4. 6 Zoomed out of electromagnetic torque result

Figure 4.6 shows the electromagnetic torque zoomed out result from the simulation time of 0.1 to 0.103 sec. Figure 4.6 also explains the structure of electromagnetic generated waveform.

4.1.3. Result of BLDC Motor Speed and State of Charge with Regenerative Braking

Figure 4.7 below shows that the output of torque, speed and state of charge during regenerative braking. From 0sec to 0.6sec the torque is positive and the speed become increasing whereas the state of charge become decreasing or discharging. Since the torque is positive and speed also positive in this time the BLDC motor is in motoring mode in quadrant one. From 0.7sec to 1.25sec the torque is negative and speed is positive but it is decreasing and state of charge is increasing.in this case the motor act as regenerative braking. The battery starts to increase its charge content and during this case the back emf is smaller than the source voltage. Energy stored is more in the battery during this regenerative condition. Generally, from the result of Figure 4.7 the speed and charging condition are inversely proportional to each otherwise when the speed is increasing the battery become is charged and as the speed is decreasing the battery starts to charge and energy become increase or reused with reducing energy losses.

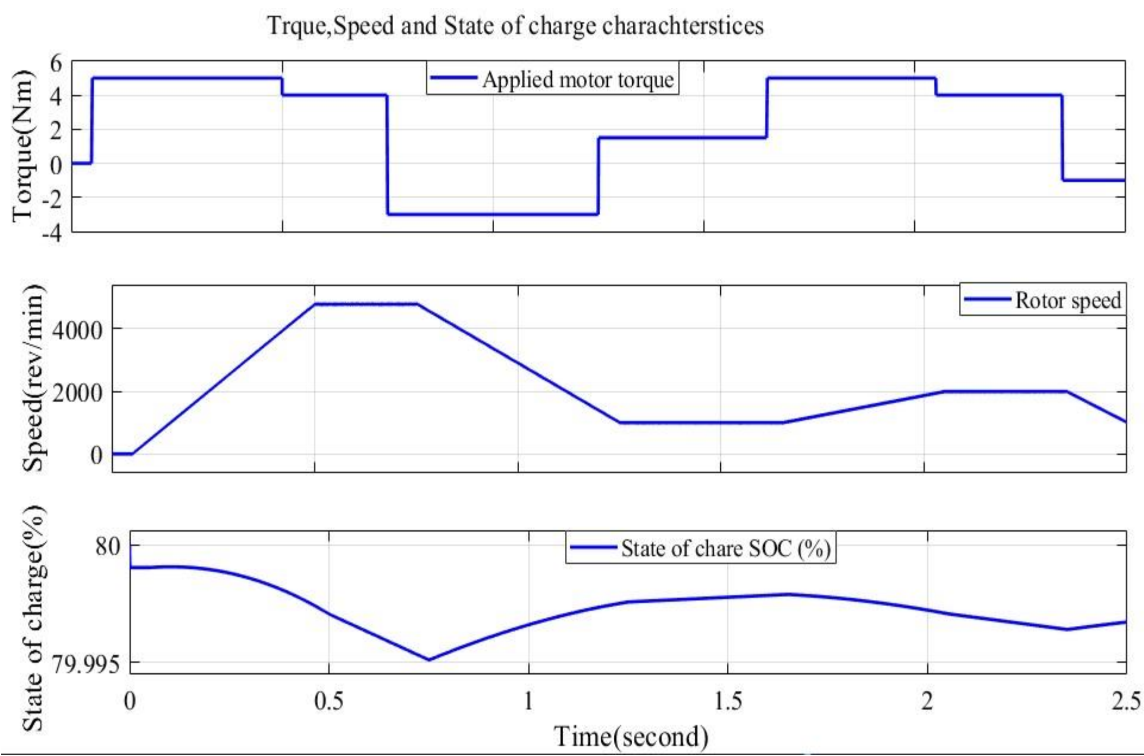

Figure 4. 7. Response of applied torque, speed and state of charge

4.1.4. Result of BLDC Motor State of charge and current with Regenerative Braking

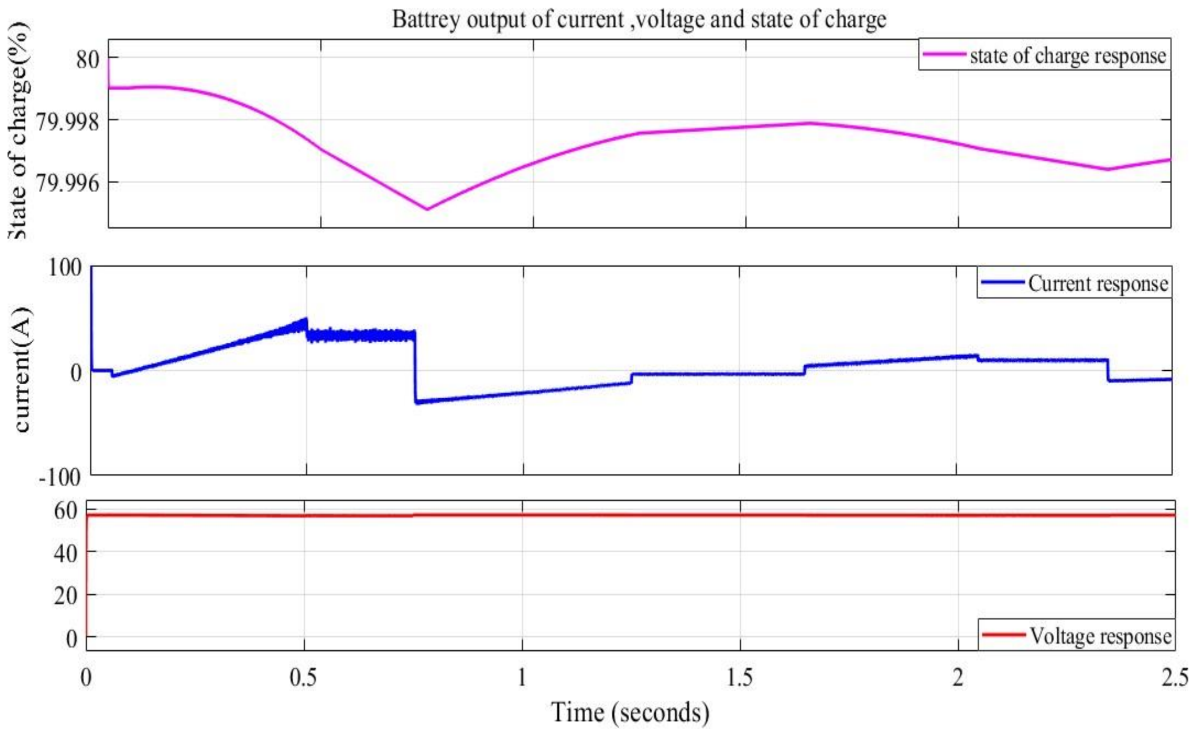

Figure 4. 8. Output response of current, voltage and state of charge

From Figure 4.8, the relationship between current and state of charge is clearly understandable. From 0sec to 0.75sec state of charge become decreasing with positive magnitude and current is increasing and positive magnitude. But from 0.75sec the state of charge starts to increase and the current become increasing with negative magnitude. When in this case the battery starts to charge and the motor operates in regenerative braking.in the two conditions the voltage in the battery is constant as shown in the red line.

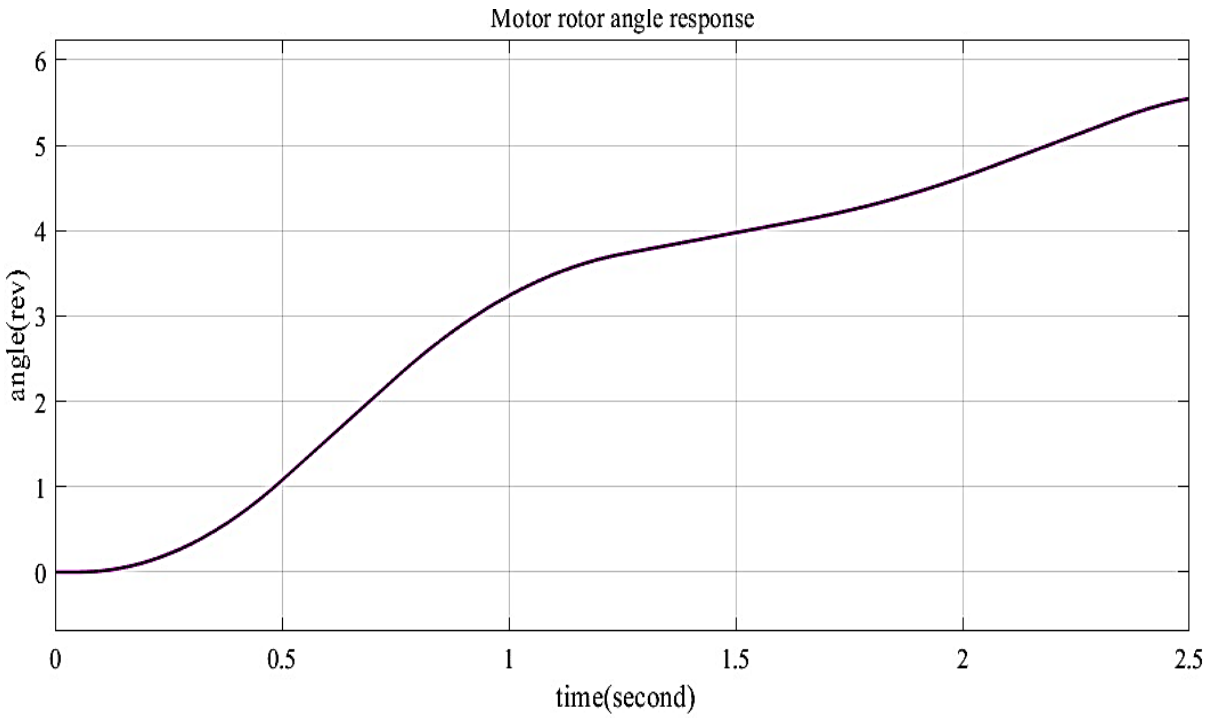

Figure 4. 9. Motor rotor Angele

Figure 4.9 is the rotor angle of BLDC motor. even if the rotor speed has different path the rotor angle has smooth path. This makes the vehicle to move in safe condition with the passenger.

CHAPTER FIVE

5. CONCLUSIONS AND RECOMMENDATIONS

5.1. Conclusions

The research work presented in this thesis can be divided into two main parts. The first part is mathematical modeling of the brushless DC (BLDC) motor and controls its speed using PSO-PID. The second part comprises the simulation results of the BEV regenerative braking, and it was charging the battery when barking is applied at the starting and stopping of the vehicle. This thesis introduced PSO as intelligent tools for tuning of PID controller. The PSO methods for the tuning of PID – controller for speed control of a BLDC motor. Obtained through simulation of BLDC motor, the simulation results show that the proposed controller can perform an efficient search for the optimal gains of PID controller. The PSO technique, it shows that, from point of view decreasing the steady state-error, settling time and peak time. While from point of view decreasing the max. Overshoot and good performance of speed tracking control. It is clearly shown that PSO tuned PID controller has better speed regulation and performance than the conventional PID controller for the same operating conditions.

The simulation studies were conducted to evaluate the performance of both proportional integral controller and PSO-PID speed control method. The advantages of this proposed method are excellent speed control, smooth transition between the quadrants and efficient conservation of energy. The BLDC motor is fed by a lithium battery via bidirectional DC-DC converter, the vehicle dynamics is considered. The two modes of operation motor and generator are explained and the designed system has only one direction of rotation, but allows regenerative braking. The simulation results show that the speed regulator gives good performance on the speed tracking, accuracy and the rejection of disturbance load. The mode generator operating permits to transform the kinetic energy in electrical energy which is stored in the battery and useful to resolve the problems relevant to the battery energy storage system and increase the autonomy of the vehicle. In this thesis, the regenerative braking concepts has been studied and implemented in MATLAB/SIMULINK. The driver block simulates a driver by pressing the accelerator pedal to drive and brake pedal to stop the car. Depending on the position or the amount of depression of the pedals certain torque is applied. Maximum brake torque applied is calculated considering the wheel dynamics. In the initial phase of brake application, when the brake torque requested is small, and then I find only the regenerative braking. Once the brake pedal has been depressed further signaling a bigger deceleration, then friction brakes comes into play in combination with regenerative braking to aid in stopping the vehicle. Some of the other limitations in terms of regeneration is the state-of-charge of the battery pack and the regenerative capability of electric motor-generator and the configurations (in-wheel motor, front driven, rear driven, all-wheel drive etc.). In order to prolong battery life, it is advised not to over-charge or undercharge the battery. Hence at times when Battery State of Charge (SOC) is at maximum limit, regeneration is not possible. In such case I could either let regeneration continue but instead of feeding it into the battery I simply have to burn it off using resistors or employ full friction braking.

5.2. Recommendations

Finally, it recommends that for anyone who wants to continue this thesis can do the implementation. This thesis is mainly focus on the PSO-PID controller so for further implementation. Different types of motors can be employed for EV use. The prominent ones can be listed as induction motor, permanent magnet synchronous motor, and synchronous reluctance motor. To add current control function to the proposed speed controller in order to keep the current within a certain range for a specific speed, could be a work for future. The proposed future work would thereby enhance the motor start-up current, reduce the motor current ripples and overall enhance the motor torque characteristics performance. The following points are candidates for investigation in the near future

- Implementation of an adaptive fuzzy logic control technique for brushless motor control.
- Applying the Ant Colony optimization approach in the tuning of PID controller.
- Adapting sophisticated control strategies such as neural network and neuro fuzzy control techniques.

REFERENCES

[1] K. R. Ed, *Brakes, Brake Control and Driver Assistance Systems*. 2014.

[2] A. Karki, S. Phuyal, D. Tuladhar, S. Basnet, and B. P. Shrestha, “Status of pure electric vehicle power train technology and future prospects,” *Appl. Syst. Innov.*, vol. 3, no. 3, pp. 1–28, 2020, doi: 10.3390/asi3030035.

[3] L. Q. Jin, Y. Zheng, J. H. Li, and Y. L. Liu, “A study of novel regenerative braking system based on supercapacitor for electric vehicle driven by in-wheel motors,” *Adv. Mech. Eng.*, vol. 7, no. 3, pp. 1–12, 2015, doi: 10.1177/1687814015573762.

[4] D. K. Sandilya, S. Goswami, B. Kalita, and S. Chakraborty, “A study on regenerative braking system with Matlab simulation,” *Proc. 2017 Int. Conf. Intell. Comput. Control. I2C2 2017*, vol. 2018-Janua, pp. 1–6, 2018, doi: 10.1109/I2C2.2017.8321879.

[5] A. Mansour, C. Mohamed Hedi, and B. Faouzi, “Experimental Study of a Pack of Supercapacitors Used in Electric Vehicles,” *Sci. World J.*, vol. 2017, 2017, doi: 10.1155/2017/6702838.

[6] M. C. Joshi, “Modeling and Control of Bidirectional DC DC Converter Fed PMDC Motor Master of Technology Modeling and Control of Bidirectional DC DC Converter Fed PMDC Motor,” no. May 2013, pp. 17–23, 2013.

[7] F. Un-Noor, S. Padmanaban, L. Mihet-Popa, M. N. Mollah, and E. Hossain, “A comprehensive study of key electric vehicle (EV) components, technologies, challenges, impacts, and future direction of development,” *Energies*, vol. 10, no. 8, 2017, doi: 10.3390/en10081217.

[8] F. Un-noor, S. Padmanaban, and L. Mihet-popa, “A Comprehensive Study of Key Electric Vehicle (EV) Components , Technologies , Challenges , Impacts , and Future Direction of Development,” pp. 1–82, 2017, doi: 10.3390/en10081217.

[9] Q. Huang, J. Li, and Y. Chen, *Control of Electric Vehicle*, no. September. 2010.

[10] A. A. Abulifa, R. K. Raja Ahmad, A. Che Soh, M. A. M. Radzi, and M. K. Hassan,

"Modelling and simulation of battery electric vehicle by using MATLAB-Simulink," *IEEE Student Conf. Res. Dev. Inspiring Technol. Humanit. SCOReD 2017 - Proc.*, vol. 2018-Janua, pp. 383–387, 2018, doi: 10.1109/SCORED.2017.8305360.

[11] J. Larminie, *Electric Vehicle Technology Explained*. .

[12] Siva Rama Prasanna Mantravadi, "Powered Electric and Plug-in Hybrid Vehicles," p. 137, 2011.

[13] M. Merugumalla, N. K.-I. journal of Applied, and undefined 2017, "Optimized PID controller for BLDC motor using Nature-inspired Algorithms," *Ripublication.Com*, vol. 12, no. 1, pp. 415–422, 2017, [Online]. Available: http://www.ripublication.com/ijaerspl2017/ijaerv12n1spl_56.pdf.

[14] D. Torres, A. Engineer, P. Heath, M. Manager, and H. M. Division, "Regenerative Braking of BLDC Motors scheme."

[15] N. Qin, "Electric Vehicle Architectures Powertrain Solutions for a Better Future," pp. 1–39, 2016.

[16] G. Luthra, "COMPARISON OF CHARACTERISTICS OF VARIOUS MOTOR DRIVES CURRENTLY USED IN ELECTRIC VEHICLE PROPULSION SYSTEM," pp. 5–8, 2017.

[17] *ELECTRIC VEHICLE MACHINS AND DRIVES*. 2015.

[18] L. Lu, X. Han, J. Li, J. Hua, and M. Ouyang, "A review on the key issues for lithium-ion battery management in electric vehicles," *J. Power Sources*, vol. 226, pp. 272–288, 2013, doi: 10.1016/j.jpowsour.2012.10.060.

[19] A. Ag, "2.1 – Vehicle and component specifications," no. 824250, 2020.

[20] U. E. D. E. Campinas, "Faculdade de Engenharia Elétrica e de Computação Study of Electric Vehicle Modeling and Strategy of Torque Control for Regenerative and Anti-lock Braking Systems Marina Gabriela Sadith Pérez Paredes Study of Electric Vehicle Modeling and Strategy of Torqu," 2018.

[21] B. M. W. Ah, “Technical specifications . BMW i3 (120 Ah).,” 2018.

[22] H. Hu, T. Wang, S. Zhao, and C. Wang, “Speed control of brushless direct current motor using a genetic algorithm–optimized fuzzy proportional integral differential controller,” *Adv. Mech. Eng.*, vol. 11, no. 11, pp. 1–13, 2019, doi: 10.1177/1687814019890199.

[23] S. Swain and B. Kumar, “Controller Design for Closed Loop Speed Control of BLDC Motor Controller Design for Closed Loop Speed Control of BLDC Motor,” no. May, 2017, doi: 10.15676/ijeei.2017.9.1.10.

[24] I. Anshory, I. Robandi, and Wirawan, “Monitoring and optimization of speed settings for Brushless Direct Current (BLDC) using Particle Swarm Optimization (PSO),” *Proc. - 2016 IEEE Reg. 10 Symp. TENSYMP 2016*, pp. 243–248, 2016, doi: 10.1109/TENCONSpring.2016.7519412.

[25] A. Tashakori and M. Ektesabi, “Comparison of different PWM switching modes of BLDC motor as drive train of electric vehicles,” *World Acad. Sci. Eng. …*, vol. 6, no. 7, pp. 594–600, 2012, [Online]. Available: http://www.waset.org/publications/10432.

[26] K. Ye and P. Li, “A new adaptive PSO-PID control strategy of hybrid energy storage system for electric vehicles,” *Adv. Mech. Eng.*, vol. 12, no. 9, pp. 1–15, 2020, doi: 10.1177/1687814020958574.

[27] M. Nasri, H. Nezamabadi-Pour, and M. Maghfoori, “A PSO-based optimum design of PID controller for a linear brushless DC motor,” *World Acad. Sci. Eng. Technol.*, vol. 26, no. 40, pp. 211–215, 2007.

[28] O. J. Oguntoyinbo, “Pid Control of Brushless Dc Motor and Robot Trajectory Planning and Simulation With,” 2009.

[29] Z. Pan, H. Bao, F. Pan, and C. Xu, “An intelligent vehicle based on an improved PID speed control algorithm for driving trend graphs,” *Int. J. Simul. Syst. Sci. Technol.*, vol.

[30] Hoda Marefat, “New Energy Management Systems for Battery Electric Vehicles with Supercapacitor,” 2019.

[31] Debajit Kumar Sandilya, Siddhartha Goswami, Bubumani Kalita, and Shweta Chakraborty, "A study on Regenerative braking system with Matlab simulation," *International Conference on Intelligent Computing and Control*, 2017.

[32] Amritha Anand, Nandan.G, and Najma.Habeeb, "A Novel Method of Energy Regeneration in Electric Vehicle," *International Journal of Innovative Research in Electrical, Electronics, Instrumentation and Control Engineering*, Vol.1, Issues 2, March 2018.

[33] D. Kavitha, Dr. A. Amudha, and S. Divyapriya, "Design of a Controller for Regenerative Braking Using BLDC Motor Applicable for Electric Vehicle," *International Journal of Electronics, Electrical and Computational System, vol.6,Issues 9, September 2017.*

[34] https://www.bmw.co.uk/en/all-models/bmw-i/i3/2020/highlights.html

[35] https://www.seeedstudio.com/blog/2019/04/01/choosing-the-right-motor-for- your-project-dc-vs-steppervsservomotors/?__cf_chl_captcha_tk=pmd_sAjFVJs6xrETUy yMT79B1vZoEjsm_kCqOTp77hl4rJU-1630177799-0-gqNtZGzNAyWjcnBszQg9

Appendixes

Appendix A: Appendixes related to analysis of data

A.1.MATLAB code for the analysis of aerodynamics dragging force versus speed of the car in Km/hr (Figure 3.4)

```
clear all; close all;
m=1500; fric=0.01; g=9.81; a=1;
r=0.25324; % Radius of the wheel in meter
K_friction=0.01; %Coefficient of friction by considering the asphalt road
F_tot=0; v=16.67; %speed of the rotor in m/se=60km/h
Tot_effcen.M=0.95;
Adnsty=1.2; %Kd/m3
Af=2; %area in m2
vo=0; %air velocity in m/s
Cw=0.2;
%Initial condition
Vkph=0;
Vkph1=0;
d_Vkph=1e-2; %unit step increment
Vkph_final=130; %final value in km/hr.
x=1;
n=1;
while(Vkph<Vkph_final),
Vmps=Vkph*(1000/3600);
Fadyna=0.5*Adnsty*Cw*Af*(Vmps+vo)^2;
if Vkph<=100*d_Vkph;
statfric=0.2;
else
statfric=0;
end
```

```
F_tot=m*g*(K_friction+statfric)+Fadyna+m*a; % Total force(Nm)
Power=F_tot*Vmps/0.95; % Required input power (Watt)
Torque=(Power*r/Vmps);% Nm
Vkph=Vkph+d_Vkph;
Vkph1=Vkph1+d_Vkph;
if x>16,
F_totn(n)=F_tot;
Torquen(n)=Torque;
Powern(n)=Power/1000; %Power in KW
Fadynan(n)=Fadyna;
Vkphn(n)=Vkph;
n=n+1;
x=1;
end
x=x+1;
end
figure();
plot(Vkphn,Fadynan,'r');
axis([0 130 0 350]);
grid
xlabel('Speed of the car(Km/hr)')
ylabel('Aerodynamic dragging force (N)')
```

A.2.MATLAB code for the analysis motive force versus approaching angle of the vehicle (Figure 3.5)

```
clear all; close all;
m=1345; fric=0.01; g=9.81; a=0.95; r=0.3; K_friction=0.01; F_tot=0; vkph=100;
Tot_effcen.M=0.93; Adnsty=1.2; Af=2.38; vo=20; Cw=0.299; apangle=0; apangle1=0;
d_apangle=1e-3;
apangle_final=10; x=1;n=1;
while(apangle<apangle_final)
```

```
vmps=vkph*(1000/3600);
theta=apangle*(2*pi/360);
FA=0.5*Adnsty*Cw*Af*(vmps-vo)^2;
if apangle<=100*d_apangle
statfric=0.001;
else
 statfric=0;
end
Frolling=m*g*(K_friction+statfric)*cos(theta);
Fgradient=m*g*sin(theta);
Fwind=Cw*Af*(vo)^2;
F_tot=Frolling+Fgradient+FA+m*a+Fwind; % Total force (Nm)
apangle=apangle+d_apangle;
apangle1=apangle1+d_apangle;
if x>17.7
F_totn(n)=F_tot;
Fgradientn(n)=Fgradient;
Frollingn(n)= Frolling; %Power in KW
FAn(n)=FA;
Fwindn(n)= Fwind;
apanglen(n)=apangle;
n=n+1; x=1;
end
x=x+1;
end
% Figure(1)
plot(apanglen, F_totn,'k',apanglen,Fgradientn,'b--
',apanglen,Frollingn,'k:',apanglen,FAn,'r',apanglen,Fwindn,'s--')
axis([0 10 0 0 10000]);
grid
xlabel('Approaching angle')
```

```
ylabel('Motive forces (N)'
```

A.3.MATLAB code for the analysis motive force versus approaching angle of the vehicle (Figure 3.6)

```
clear all; close all;
m=1345; % Mass of the car
fric=0.01; %Friction coefficient
g=9.81; %gravitational acceleration
a=0.5; % Acceleration (m/sec)
r=0.25324; % Radius of the wheel in meter
K_friction=0.01; %Coefficient of friction by considering the asphalt road
F_tot=0;
vkph=100; % Speed of the rotor in Km/hr
Tot_effcen.M=0.95; %Efficiency
Adnsty=1.2; %Kd/m3
Af=2.83; % Frontal area of the car (m2)
vo=15; %Air velocity in m/s
Cw=0.2;
%Initial condition
apangle=0;
apangle1=0;
d_apangle=1e-2; %unit step increment
apangle_final=30; %final value in degree
x=1;n=1;
while(apangle<apangle_final),
vmps=vkph*(1000/3600);
theta=apangle*(2*pi/360);
FA=0.5*Adnsty*Cw*Af*(vmps+vo)^2;
if apangle<=100*d_apangle;
statfric=0.001;
else
```

```
    statfric=0;
end
Frolling=m*g*(K_friction+statfric)*cos(theta);
Fgradient=m*g*sin(theta);
F_tot=Frolling+Fgradient+FA+m*a; % Total force (Nm)
apangle=apangle+d_apangle;
apangle1=apangle1+d_apangle;
if x>16,
F_totn(n)=F_tot;
Fgradientn(n)=Fgradient;
Frollingn(n)= Frolling; %Power in KW
FAn(n)=FA;
apanglen(n)=apangle;
n=n+1;
x=1;
end
x=x+1;
end
figure(1);
plot(apanglen, F_totn,'k',apanglen,Fgradientn,'b--',apanglen,Frollingn,'k:',apanglen,FAn,'r')
axis([0 30 0 9000]);
grid
xlabel('Approaching angle')
ylabel('Motive forces (N)')
```

A.4.MATLAB code for the analysis driving power vs speed of the electric vehicle (Figure 3.7)

```
clear all;
close all;
m=1345; % mass of the Vehicle
fric=0.01; g=9.81;
```

```
a=0.95; % acceleratin in m/s^2
r=0.3; % Radius of the wheel in meter 1142/70-R12
K_friction=0.01; %Coefficient of friction by considering asphalt road
F_tot=4175.3;
v=41.67; %speed of the car in m/s
Tot_effcen.M=0.93;
Adnsty=1.2; %air density Kg/m^3
Af=2.38; %area in m^2
vo=20; %air velocity in m/s
Cd=0.299; % drag coefficient
%Initial condition
Vkph=0;
Vkph1=0;
d_Vkph=1e-2; %unit step increment
Vkph_final=160; %final value in km/hr.
x=1;
n=1;
while(Vkph<Vkph_final),
   Vmps=Vkph*(1000/3600);
Fadyna=0.5*Adnsty*Cd*Af*(Vmps-vo)^2;
fwind=Cd*Af*(vo)^2;
if Vkph<=1000*d_Vkph;
statfric=0.01;
else
   statfric=0;
end
F_tot=m*g*(K_friction+statfric)+Fadyna+m*a+fwind; % Total force(Nm)
Power=F_tot*Vmps/0.93; % Required input power (Watt)
Torque=(Power*r/Vmps);% Nm
Vkph=Vkph+d_Vkph;
Vkph1=Vkph1+d_Vkph;
```

```
if x>17.77,
   F_totn(n)=F_tot;
Torquen(n)=Torque;
Powern(n)=Power/1000; %Power in KW
Fadynan(n)=Fadyna;
Vkphn(n)=Vkph;
n=n+1;
x=1;
end
x=x+1;
end
plot(Vkphn,Powern,'r','LineWidth',1.5);
set(gca,'FontSize',12)
axis([0 160 0 120]); grid
xlabel('Speed of the of the car(Km/hr)')
ylabel('Power (KW)')
```

A.5.MATLAB code for torque versus speed characteristics curve (Figure 3.)

```
clear all
Ratedpower=75000; %Rated power in Watt
wrpm=0; %initial condition
wb= 230.266666667; %base speed in rad/sec
d_wrpm=1e-2; %unit step increment
wrpm_final=4800; %final value in RPM
x=1;
n=1;
while(wrpm<wrpm_final),
wm=wrpm*(2*pi)/60;
Torque= Ratedpower/wm;
if Torque>= 250,
Torque= 250;
```

```
end
if Torque<250,
Torque= Torque;
end
Power=Torque*wm;
wrpm=wrpm+d_wrpm;
 if x>17.77,
wrpmn(n)=wrpm;
Torquen(n)=Torque;
Powern(n)=Power/1000;
n=n+1;
x=1;
end
x=x+1;
end
figure(1);
[AX,Torque,Power]=plotyy(wrpmn,Torquen, wrpmn,Powern);
axis([0 8000 0 350 ]);
set(get(AX(1),'ylabel'), 'string','Motor torque in Nm')
set(get(AX(2),'ylabel'), 'string','Motor power kW')
set(Torque,'LineStyle','--')
set(Power,'LineStyle','-')
set(gca, 'FontName','TimesNewRoman')
set(gca, 'FontSize',12)
set([Torque,Power],'LineWidth',1)
xlabel('Motor speed in rpm')
grid on
legend('Motor torque','Motor power')
```

A.6.MATLAB code for analysis of the effect of the approaching angle in the power of the vehicle (Figure 3.9)

```
clear all; close all;
m=1345; fric=0.01; g=9.81; a=0; r=0.3; c_ofriction=0.01; d=0.3; v=41.67;
Tot_effcen.M=0.93; Adnsty=1.2; Af=2.38; vo=20; Cw=0.299; angleR=0; angleR1=0;
d_angleR=1e-6;
angleR_final=25; x=1; n=1;
while(angleR<angleR_final),
Fadyna=0.5*Adnsty*Cw*Af*(v-vo)^2;
fwind=Cw*Af*(vo)^2;
theta=angleR*2*pi/360; %Degree to radian conversion
F_tot=m*g*(sin(theta)+c_ofriction*cos(theta))+Fadyna+m*a+fwind; % Total force(Nm)
Power=F_tot*v; Torque=(Power*r/v)/0.93;
angleR=angleR+d_angleR;
angleR1=angleR1+d_angleR;
if x>17,
F_totn(n)=F_tot;
Torquen(n)=Torque; Powern(n)=Power/1000; %Power in KW
Fadynan(n)=Fadyna;
```

Appendix B: MATLAB/Simulink Model for the Proposed System

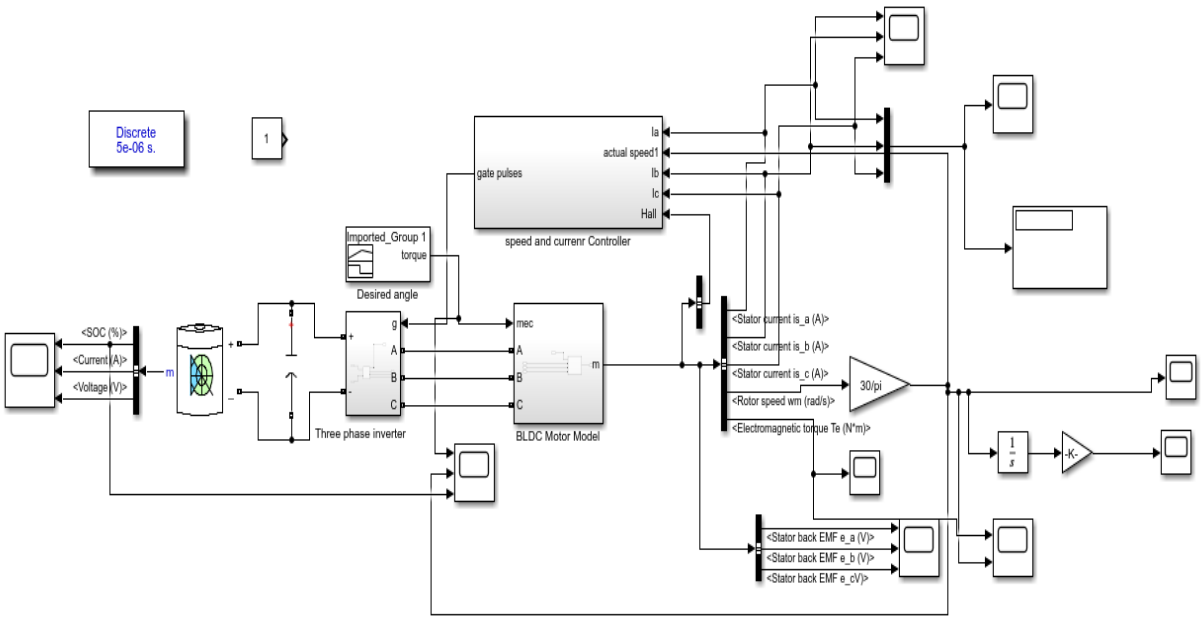

Figure B. 1.Overall system Simulink model

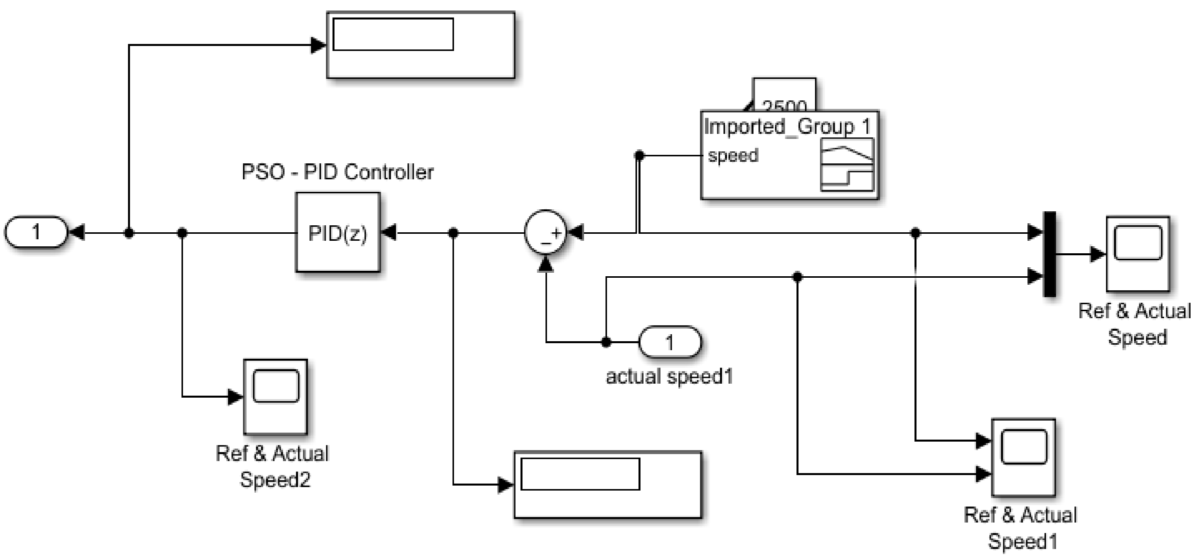

Figure B. 2.PSO-PID speed controller

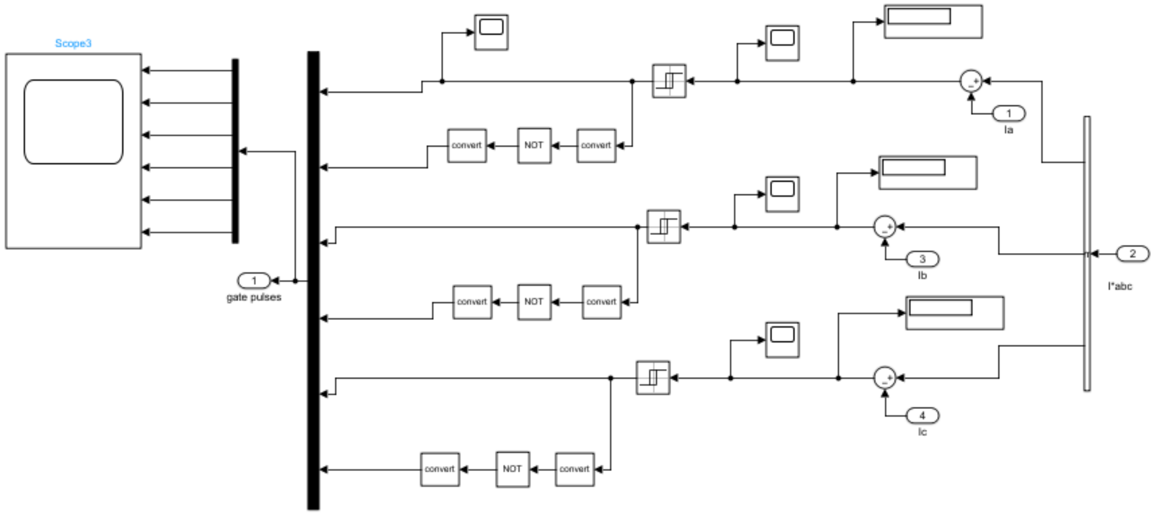

Figure B. 3.Hysteresis current controller

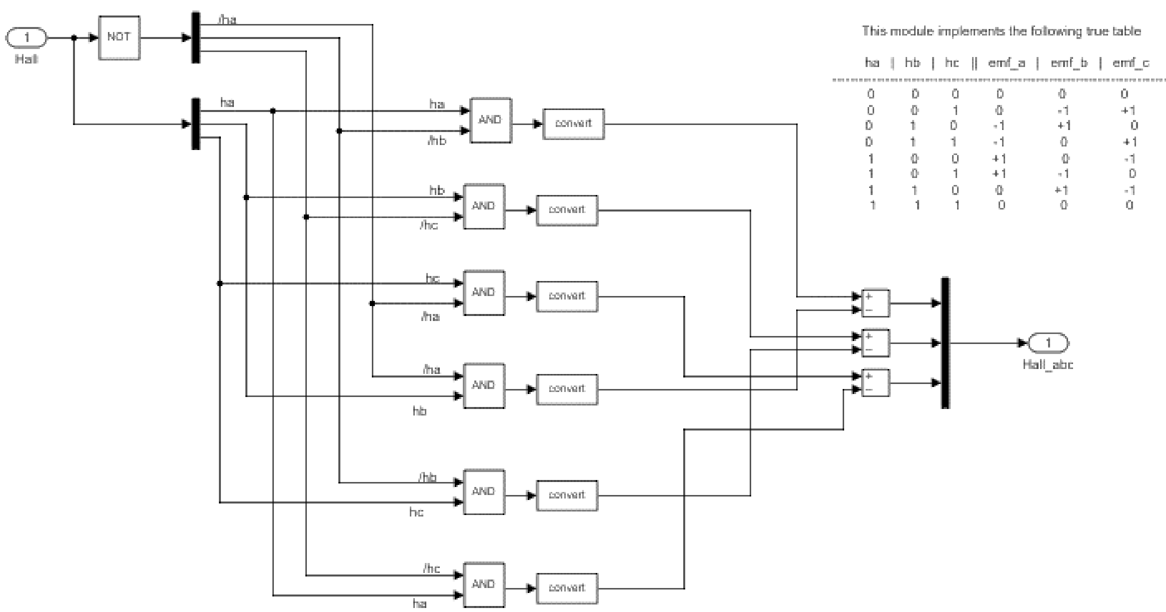

ha	hb	hc	emf_a	emf_b	emf_c
0	0	0	0	0	0
0	0	1	0	-1	+1
0	1	0	-1	+1	0
0	1	1	-1	0	+1
1	0	0	+1	0	-1
1	0	1	+1	-1	0
1	1	0	0	+1	-1
1	1	1	0	0	0

Figure B. 4.Commutation logic from hall sensor

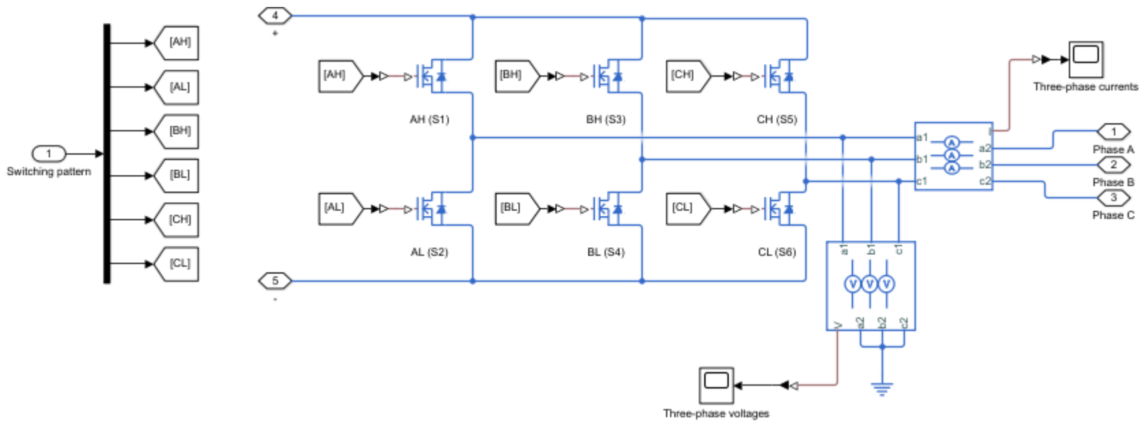

Figure B. 5.Three phase inverter

Appendix C: Appendixes related to data collection

Data from internet: Data of similar size motor used for EV (accessed on April 09, 2021).

Power	The battery	voltage	Speed	Rated torque	Peak torque	Peak power	current	Peak current	Efficiency	Weight
50KW	360V	540V	3500rpm	136Nm	300Nm	110KW	140A	320A	95.4%	250kg
60KW	360V	540V	3500rpm	164Nm	350Nm	130KW	172A	380A	95.6%	260kg
75KW	360V	540V	3500rpm	205Nm	260Nm	160KW	212A	430A	95.7%	270kg
100KW	380V	540V	5000rpm	191Nm	400Nm	220KW	289.3A	590A	96.0%	270kg